

Local Causal Discovery for Structural Evidence of Direct Discrimination

Jacqueline Maasch¹, Kyra Gan¹, Violet Chen², Agni Orfanoudaki³, Nil-Jana Akpınar^{4†}, Fei Wang⁵

¹Cornell Tech

²Stevens Institute of Technology

³University of Oxford

⁴Amazon AWS AI/ML

⁵Weill Cornell Medicine

Abstract

Identifying the causal pathways of unfairness is a critical objective in improving policy design and algorithmic decision-making. Prior work in causal fairness analysis often requires knowledge of the causal graph, hindering practical applications in complex or low-knowledge domains. Moreover, global discovery methods that learn causal structure from data can result in unstable performance with finite samples, potentially leading to contradictory fairness conclusions. To mitigate these issues, we introduce *local discovery for direct discrimination* (LD3): a method that uncovers structural evidence of direct discrimination by identifying the causal parents of an outcome variable. LD3 performs a linear number of conditional independence tests relative to variable set size, and allows for latent confounding under the sufficient condition that no parent of the outcome is latent. We show that LD3 returns a valid adjustment set (VAS) under a new graphical criterion for the *weighted controlled direct effect*, a qualitative indicator of direct discrimination. LD3 limits unnecessary adjustment, providing interpretable VAS for assessing unfairness. We use LD3 to analyze causal fairness in two complex decision systems: criminal recidivism prediction and liver transplant allocation. LD3 was more time-efficient and returned more plausible results on real-world data than baselines, which took $46\times$ to $5870\times$ longer to execute.

1 Introduction

Fairness holds fundamental importance in policy design and algorithmic decision-making, especially in high-stakes domains such as healthcare and policing (Starke et al. 2022; Corbett-Davies et al. 2023). Various criteria have been proposed for measuring unfairness with respect to protected or sensitive attributes, such as gender and ethnicity (Verma and Rubin 2018). Legal doctrines generally differentiate between direct discrimination and indirect or spurious forms of unfairness, codifying the notion that the *mechanism* of unfairness matters (Barocas and Selbst 2016; Carey and Wu 2022). However, fairness criteria based solely on statistical associations cannot disentangle these mechanisms (Kilbertus et al. 2017; Makhlof, Zhioua, and Palamidessi 2020), limiting their informativeness and actionability for policy interventions. Consequently, there is a growing emphasis on applying causal reasoning in fairness (Kilbertus et al.

2017), shifting the focus from associations to interventions and counterfactual outcomes (Bareinboim et al. 2022).

Causal fairness analysis (CFA) provides a theoretical framework for disentangling the mechanisms of unfairness using the language of *structural causal models* (SCMs). Previous works in CFA (Zhang and Bareinboim 2018; Plecko and Bareinboim 2023) and the allied field of mediation analysis (Pearl 2001; Vanderweele 2011; Shpitser and VanderWeele 2011; Pearl 2014) generally assume significant prior structural knowledge to decompose direct, indirect, and spurious effects. In practice, structural knowledge is often incomplete, absent, or contentious for complex domains, even among experts (Petersen et al. 2023). Furthermore, the *identifiability* of multiple proposed measures of direct and indirect effects has been a topic of extensive debate among theoreticians (Pearl 2014), raising barriers to entry for applied researchers (Vanderweele 2011). Thus, existing methodologies in CFA can be difficult to apply in complex systems.

Among the many fairness measures proposed in CFA, the *controlled direct effect* (CDE) is a relatively straightforward qualitative indicator of direct discrimination that takes non-zero values only when the exposure is a direct cause of the outcome (Zhang and Bareinboim 2018). As the CDE is more interpretable for real-world interventions than other direct effect measures (VanderWeele 2013), requires fewer untestable assumptions over the data generating process (Shpitser and VanderWeele 2011), and requires less prior structural knowledge (Pearl 2001), it has been used to assess direct effects in policy evaluation (Vanderweele 2011; VanderWeele 2013) and epidemiology (Vansteelandt 2009). To increase the practicality of CFA in complex domains, we choose to focus on the CDE as a starting point for this work.

In low-knowledge domains, we can support CFA by learning causal structure directly from observational data. However, *global causal discovery* from finite data samples is challenging due to high sample complexity (Spirtes et al. 2001) and exponential time complexity in unconstrained search spaces (Chickering 2002; Chickering, Heckerman, and Meek 2004; Claassen, Mooij, and Heskes 2013). Learned causal graphs often disagree with expert knowledge in complex domains (Shen et al. 2020; Petersen et al. 2023), and can yield conflicting causal fairness conclusions in CFA (Binkytė et al. 2023 and Section 6 of this paper).

While global discovery learns the relations among all ob-

Preprint. [†]Work done outside of Amazon. Corresponding author J. Maasch: maasch@cs.cornell.edu.

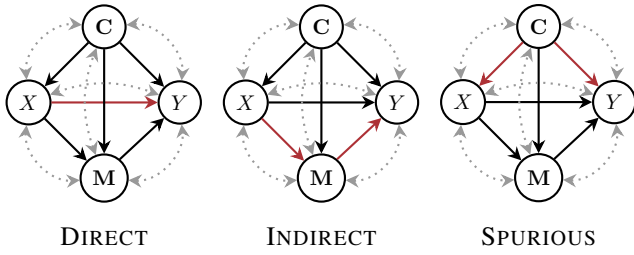


Figure 1: The *standard fairness model* is compactly represented as a local subgraph around protected attribute X and outcome Y (Plečko and Bareinboim 2024). Variables that are irrelevant to CFA are abstracted away, leaving confounders (C) and mediators (M). Directed edges represent the existence of active directed paths, and bidirected edges denote potential confounding. This work aims to identify *direct* mechanisms of unfairness in a data-driven way.

served variables, *local causal discovery* (Gao and Ji 2015; Cai et al. 2023; Dai et al. 2024) only learns the substructures relevant for downstream tasks, such as causal effect estimation (Shah, Shanmugam, and Ahuja 2022; Cheng et al. 2022; Gupta, Childers, and Lipton 2023; Maasch et al. 2024; Shah, Shanmugam, and Kocaoglu 2024) or feature selection (Yu et al. 2021; Yu, Liu, and Li 2021). As the *standard fairness model* (SFM; Figure 1) is represented as a local subgraph surrounding an attribute and outcome of interest (Plečko and Bareinboim 2024), local discovery offers a natural framework for CFA. However, since task-specific local discovery algorithms are definitionally one-size-does-not-fit-all, existing methods may not be optimal for fairness tasks.

Contributions This work aims to increase the practicality of CFA for direct discrimination in complex domains with unknown causal graphs. Our contributions are three-fold.

1. **Local discovery for direct discrimination (LD3)**. This local causal discovery method leverages the problem structure in CFA to efficiently detect graphical signatures of direct discrimination.¹ LD3 discovers the parents of an outcome variable in a linear number of independence tests with respect to variable set size, guaranteeing correctness under sufficient conditions.
2. **A graphical criterion for the weighted controlled direct effect (WCDE)**. This criterion is sufficient to identify a valid adjustment set (VAS) for the WCDE, a qualitative indicator of direct discrimination. This criterion is satisfied by the knowledge returned by LD3.
3. **Real-world fairness analysis**. We deploy LD3 for two fairness problems: (1) racial discrimination in recidivism prediction and (2) sex-based discrimination in liver transplant allocation. LD3 recovered more plausible causal relations than local and global baselines, which performed $11\text{--}1021\times$ more tests and took $46\text{--}5870\times$ longer to run.

Paper Structure Section 2 defines essential concepts in CFA and direct effect estimation. In Section 3, we introduce

¹Code on GitHub:

<https://anonymous.4open.science/r/LD3-4440>

LD3 and describe our methodological contributions. Section 4 contextualizes our work in the literature. Section 5 presents numerical validation on synthetic and semi-synthetic data. Section 6 presents two real-world fairness analyses.

2 Preliminaries

Let univariate random variables be denoted by capital letters (e.g., X), with specific values in lowercase (e.g., $X = x$). Multivariate random variables or sets are denoted by bold-face capital letters (e.g., \mathbf{X}), with vector values in bold lowercase (e.g., $\mathbf{X} = \mathbf{x}$). Graphs or function sets are denoted by calligraphic letters (e.g., \mathcal{F}). Let $pa(\cdot)$, $an(\cdot)$, $ch(\cdot)$, and $de(\cdot)$ denote the parent, ancestor, child, and descendant sets for a variable in causal graph \mathcal{G} , respectively.

2.1 Causal Fairness Analysis

CFA can be framed in the language of SCMs and their graphical representations (Plečko and Bareinboim 2024).

Definition 1 (Structural causal model, Pearl 2001). A SCM is a 4-tuple $\langle \mathbf{V}, \mathbf{U}, \mathcal{F}, P(\mathbf{u}) \rangle$ where $\mathbf{U} = \{U_i\}_{i=1}^n$ denotes a set of exogenous variables determined by factors outside of the model, $\mathbf{V} = \{V_i\}_{i=1}^n$ denotes a set of observed endogenous variables determined by variables in $\mathbf{U} \cup \mathbf{V}$, $\mathcal{F} = \{f_i\}_{i=1}^n$ denotes a set of structural functions such that $V_i = f_i(pa(V_i), U_i)$, and $P(\mathbf{u})$ is the distribution over the exogenous variables \mathbf{U} .

Every SCM corresponds to a causal graphical model. To facilitate CFA, the true causal graph for an SCM can be *compactly represented* using the SFM (Figure 1).

Definition 2 (Standard fairness model (SFM), Plečko and Bareinboim 2024). Let $\mathcal{G} = (\mathbf{V}, \mathbf{E})$ be a causal graph with vertices \mathbf{V} and edges \mathbf{E} . Let \mathcal{G}_{SFM} be the *projection* of \mathcal{G} onto the SFM, which is obtained by (1) selecting a protected attribute-outcome pair $\{X, Y\} \subset \mathbf{V}$ and (2) identifying sets $\mathbf{M}, \mathbf{C} \subseteq \mathbf{V} \setminus \{X, Y\}$ that satisfy a specific set of relations with respect to $\{X, Y\}$. Thus, \mathcal{G}_{SFM} is the graph induced by $\{X, Y, \mathbf{M}, \mathbf{C}\} \subseteq \mathbf{V}$ that encodes the following:

- X is the protected attribute of interest.
- Y is the outcome of interest.
- \mathbf{M} is the set of mediators with respect to X and Y .
- \mathbf{C} is the set of confounders with respect to X and Y (i.e., any variable on a backdoor path for X and Y ; VanderWeele and Shpitser 2013).

Note that \mathbf{C} and \mathbf{M} can be empty. Central tasks in CFA are to (1) probe whether the red paths in Figure 1 exist and (2) estimate the associated effect sizes. The SFM allows for *observed or latent confounding* among $\mathbf{C}, \mathbf{M}, X, Y$ (Figure 1). In this work, we add one caveat: the sufficient (not necessary) condition that no parent of Y is latent (Section 3).

Structural Fairness Criteria Multiple criteria have been proposed for evaluating fairness from graphical structures. Here, we focus on a criterion for direct discrimination.

Definition 3 (Structural direct criterion (SDC), Plečko and Bareinboim 2024). An SCM is fair in terms of direct discrimination if and only if the protected attribute is not a par-

ent of the outcome:

$$SDC = \begin{cases} 1 & \text{if } X \text{ is a parent of } Y, \\ 0 & \text{if } X \text{ is not a parent of } Y. \end{cases} \quad (1)$$

2.2 Controlled Direct Effect

The CDE is a valid qualitative test for identifying direct discrimination, as the true value is non-zero if and only if there is a direct path from the protected attribute to the outcome (Zhang and Bareinboim 2018). Let $X = x$ and $X = x^*$ be the exposure values corresponding to treatment and no treatment (i.e., the reference value), respectively.

Definition 4 (Controlled direct effect, Vanderweele 2011). The CDE measures the expected change in outcome as the exposure changes, given covariates \mathbf{S} , when mediators \mathbf{M} are uniformly fixed to a constant value \mathbf{m} :

$$CDE(\mathbf{m}) := \mathbb{E}[Y_{x,\mathbf{m}} - Y_{x^*,\mathbf{m}}]. \quad (2)$$

Definition 5 (Identifiability conditions of the CDE, Vanderweele 2011). The CDE is identifiable from observational data when, given covariates \mathbf{S} , the following holds for all values $X = x$ and $\mathbf{M} = \mathbf{m}$:

1. There is no latent confounding of the exposure and outcome given covariates \mathbf{S} , i.e., $Y_{x,\mathbf{m}} \perp\!\!\!\perp X | \mathbf{S}$.
2. There is no latent confounding of the mediators and outcome given $\{X, \mathbf{S}\}$, i.e., $Y_{x,\mathbf{m}} \perp\!\!\!\perp \mathbf{M} | X, \mathbf{S}$.

Then, $CDE(\mathbf{m})$ is identifiable as

$$\sum_{\mathbf{s}} [\mathbb{E}[Y|x, \mathbf{s}, \mathbf{m}] - \mathbb{E}[Y|x^*, \mathbf{s}, \mathbf{m}]] P(\mathbf{s}) \quad (3)$$

where fixing \mathbf{m} over the population is simulated by conditioning on \mathbf{m} (Pearl 2012a).

When *interaction* between the mediator and exposure is present, the CDE does not display *effect constancy*: the CDE will be non-unique, taking on as many values as there are levels of \mathbf{M} . Effect constancy is guaranteed for the CDE in linear systems, but not in nonlinear systems (Pearl 2014). To ease notation, assuming discrete \mathbf{M} , we define the *weighted CDE* (WCDE) as the following expectation over \mathbf{M} .²

Definition 6 (Weighted CDE over \mathbf{M}). For all values of covariates \mathbf{S} and mediators \mathbf{M} , $WCDE :=$

$$\sum_{\mathbf{m}} \sum_{\mathbf{s}} [\mathbb{E}[Y|x, \mathbf{s}, \mathbf{m}] - \mathbb{E}[Y|x^*, \mathbf{s}, \mathbf{m}]] P(\mathbf{m}) P(\mathbf{s}). \quad (4)$$

As the WCDE is a weighted sum over elements that are well-defined under the identifiability conditions in Definition 5, the WCDE is identifiable under Definition 5 as well.

Definition 7 (VAS for the WCDE). Given Definitions 5 and 6, a VAS for WCDE estimation blocks (1) all backdoor paths for $\{X, Y\}$, (2) all backdoor paths for $\{\mathbf{M}, Y\}$, and (3) all mediator paths for $\{X, Y\}$.

²Definition 6 generalizes to continuous \mathbf{M} by integrating over its possible values. We note that LD3 operates independently of the variable type of \mathbf{M} .

As a Fairness Metric By definition, $CDE(\mathbf{m}) \neq 0$ implies direct discrimination (Zhang and Bareinboim 2018). Since the WCDE is a sum, it can be zero when all elements are zero or when non-zero elements cancel out. However, it can only be non-zero if at least one $CDE(\mathbf{m}) \neq 0$. Thus, we encourage caution when interpreting zero values.

Comparison to Other Direct Effects Several estimands can capture direct effects, including CDE (Pearl 2001), natural direct effect (NDE; Pearl 2001), and counterfactual direct effect (Ctf-DE; Zhang and Bareinboim 2018). The CDE is an interventional quantity, while NDE and Ctf-DE are counterfactual quantities. We favor WCDE as a fairness metric in complex domains because it requires fewer untestable assumptions over the data generating process (Shpitser and VanderWeele 2011) and less prior structural knowledge than NDE and Ctf-DE (Pearl 2001; Vanderweele 2011; Zhang and Bareinboim 2018). The main objective of this work is to assess whether the protected attribute is a direct cause of the outcome (i.e., $X \rightarrow Y$). **The CDE, NDE, and Ctf-DE are all zero when there is no edge $X \rightarrow Y$.** Thus, we advocate for the simpler estimand for practicality. See Appendix A for an extended comparison of direct effect measures.

2.3 Mapping Causal Partitions to the SFM

To facilitate efficient structure learning, we leverage the *causal partition* taxonomy defined in Maasch et al. (2024) (Table 1). Given an exposure-outcome pair $\{X, Y\}$, any arbitrary variable set \mathbf{Z} can be uniquely partitioned into exactly eight disjoint subsets (which may be empty) that are defined by the types of causal paths that they share with X and Y . Narrowing the focus of structure learning to the relationships that are *causally relevant* to the exposure and outcome (Cai et al. 2023), this partition taxonomy provides convenient building blocks for local discovery. Mapping this partition taxonomy to the SFM, \mathbf{Z}_1 are confounders \mathbf{C} (and their proxies) and \mathbf{Z}_3 are mediators \mathbf{M} (and their proxies).³

EXHAUSTIVE, DISJOINT CAUSAL PARTITIONS W.R.T. $\{X, Y\}$	
\mathbf{Z}_1	Confounders and their proxies.
\mathbf{Z}_2	Colliders and their proxies.
\mathbf{Z}_3	Mediators and their proxies.
\mathbf{Z}_4	Non-descendants of Y where $\mathbf{Z}_4 \perp\!\!\!\perp X$ and $\mathbf{Z}_4 \not\perp\!\!\!\perp X Y$.
\mathbf{Z}_5	Instruments and their proxies.
\mathbf{Z}_6	Descendants of Y . All active paths with X are mediated by Y .
\mathbf{Z}_7	Descendants of X . All active paths with Y are mediated by X .
\mathbf{Z}_8	Nodes that share no active paths with X nor Y .

Table 1: Adapted from Maasch et al. (2024).

3 Local Discovery for Direct Discrimination

Algorithm 1 provides a constraint-based discovery method for assessing the SDC and learning a VAS for WCDE estimation from observational data. The number of independence tests performed scales linearly with the number of

³See Maasch et al. (2024) for more formal partition definitions. Proxy variables are not relevant in this setting, as we are only concerned with true confounders and mediators. Proxies cannot be parents of Y , and are not returned by LD3.

Algorithm 1: LD3: Learning structural evidence of direct discrimination from observational data.

Input: Exposure X , outcome Y , variable set \mathbf{Z} , independence test, significance level α .

Output: Adjustment set \mathbf{A}_{DE} , SDC results.

Assumptions: Sufficient conditions A1 and A2.

```

1:  $\mathbf{Z}' \leftarrow \mathbf{Z}$ 
2: for  $\forall Z \in \mathbf{Z}'$  do
3:   if  $Z \perp\!\!\!\perp X \wedge Z \perp\!\!\!\perp Y$  then  $Z \in \widehat{\mathbf{Z}}_8$ 
4:   if  $Z \not\perp\!\!\!\perp Y \wedge Z \perp\!\!\!\perp Y|X$  then  $Z \in \widehat{\mathbf{Z}}_{5,7}$ 
5:   if  $Z \perp\!\!\!\perp X \wedge Z \not\perp\!\!\!\perp X|Y$  then  $Z \in \widehat{\mathbf{Z}}_4$ 
6:  $\mathbf{Z}' \leftarrow \mathbf{Z}' \setminus \widehat{\mathbf{Z}}_8 \cup \widehat{\mathbf{Z}}_{5,7} \cup \widehat{\mathbf{Z}}_4$ 
7: for  $\forall Z \in \mathbf{Z}'$  do
8:   if  $Z \not\perp\!\!\!\perp Y|X \cup \widehat{\mathbf{Z}}_4 \cup \{\mathbf{Z}' \setminus Z\}$  then  $Z \in \widehat{\mathbf{Z}}_{1 \in pa(Y)} \cup \widehat{\mathbf{Z}}_{3 \in pa(Y)}$ 
9:   for  $\forall \widehat{\mathbf{Z}}_4 \in \widehat{\mathbf{Z}}_4$  do
10:    if  $\widehat{\mathbf{Z}}_4 \not\perp\!\!\!\perp Y|X \cup \widehat{\mathbf{Z}}_{1 \in pa(Y)} \cup \widehat{\mathbf{Z}}_{3 \in pa(Y)} \cup \{\widehat{\mathbf{Z}}_4 \setminus \widehat{\mathbf{Z}}_4\}$ 
    then  $\widehat{\mathbf{Z}}_4 \in \widehat{\mathbf{Z}}_{4 \in pa(Y)}$ 
11:  $\mathbf{A}_{DE} \leftarrow \widehat{\mathbf{Z}}_{1 \in pa(Y)} \cup \widehat{\mathbf{Z}}_{3 \in pa(Y)} \cup \widehat{\mathbf{Z}}_{4 \in pa(Y)}$ 
12: if  $X \perp\!\!\!\perp Y|\widehat{\mathbf{Z}}_{1 \in pa(Y)} \cup \widehat{\mathbf{Z}}_{3 \in pa(Y)}$  then  $SDC \leftarrow 0$ 
13: else  $SDC \leftarrow 1$ 
14: return  $\mathbf{A}_{DE}, SDC$ 

```

nodes. Proofs of correctness are in Appendix B. $\widehat{\mathbf{Z}}_{(\cdot)}$ denotes the predicted partition label of each observed variable.

Time Complexity Constraint-based discovery methods are typically analyzed by the total number of independence tests performed (Spirtes et al. 2001; Tsamardinos et al. 2006). For-loops at Lines 2–5, 7–8, and 9–10 of Algorithm 1 perform $O(|\mathbf{Z}|)$ number of tests each. All remaining lines perform a constant number of operations. Thus, the total number of independence tests is of $O(|\mathbf{Z}|)$.

Sufficient Conditions for Structure Learning We assume causal Markov, faithfulness, and acyclicity. We do not impose parametric assumptions on causal functions nor distributional forms. As for all constraint-based methods, the independence test selected may impose its own parametric assumptions. When these are not well-justified, we recommend nonparametric tests (e.g., Gretton et al. 2005, 2007; Zhang et al. 2011; Runge 2018). Asymptotic guarantees on partition correctness, SDC correctness, and valid adjustment for WCDE estimation hold under Assumptions A1 and A2.

A1 Y has no descendants in the observed variable set. This is satisfied when Y is a terminal variable in the temporal ordering (e.g., when outcome is death, or a policy or algorithmic decision made at a known time point).

A2 All parents of Y are observed. Latent variables that are not parents of Y are permissible. Thus, this is a milder condition than assuming causal sufficiency.

Note that these assumptions are sufficient but not necessary. Assumption A1 has been previously used to facilitate parent and ancestor learning (Soleymani et al. 2022; Cai et al. 2023). LD3 learns causal partitions directly from data, with-

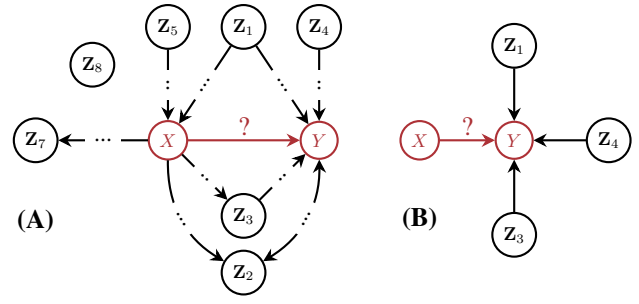


Figure 2: LD3 assesses whether the edge $X \rightarrow Y$ exists. (A) Allowable partitions under A1 and A2. (B) Parents of Y returned by LD3. Nodes are partition sets or subsets. Partition interrelations and latent confounding are abstracted away. Bidirected edge $Y \leftrightarrow Z_2$ signifies $Z_2 \notin de(Y)$. Edges with \dots are paths of arbitrary length. Solid edges are adjacencies.

out assumptions on temporal ordering other than 1) Y cannot cause X and 2) A1. Assumption A2 is a consequence of the sufficient conditions for CDE identifiability, as Definition 5 requires blocking all spurious and indirect paths from X to Y . A2 allows for unobserved variables that are not parents of Y , and is, therefore, more relaxed than the causal sufficiency typically assumed in discovery (e.g., PC (Spirtes 2001), NOTEARS (Zheng et al. 2018), NoGAM (Montagna et al. 2023), etc.). We exploit A2 to evaluate the SDC, as it ensures that X is conditionally d -separable from Y when there is no direct path from X to Y . It also ensures that no colliders in $\mathbf{Z}_{2 \notin de(Y)}$ are retained for adjustment.

We empirically demonstrate failure modes and robustness to violations of A2 in Appendix C.1, showing that A2 is sufficient but not necessary. We prove in Appendix B that latent variables not adjacent to Y do not impact correctness.

Theorem 1. Latent variables that are not parents of Y do not affect Algorithm 1.

Causal Partitions in this Setting Given A1, there are no descendants of Y in \mathcal{G} . Thus, there are no \mathbf{Z}_6 nor $\mathbf{Z}_{2 \in de(Y)}$. However, there may be $\mathbf{Z}_{2 \notin de(Y)}$. Thus, \mathcal{G} can contain the following seven (potentially empty) causal partitions with respect to $\{X, Y\}$: \mathbf{Z}_1 , $\mathbf{Z}_{2 \notin de(Y)}$, \mathbf{Z}_3 , \mathbf{Z}_4 , \mathbf{Z}_5 , \mathbf{Z}_7 , and \mathbf{Z}_8 (Figure 2.A). LD3 returns the partition subsets in Figure 2.B: all \mathbf{Z}_1 , \mathbf{Z}_3 , and \mathbf{Z}_4 that are directly adjacent to Y .

Remark 1 (The observed WCDE under violations of A2). While A2 is sufficient and *not necessary* for WCDE identifiability, each backdoor and frontdoor path must be blocked by at least one observable variable. If no variables on a given backdoor or frontdoor path are measured, it is possible that $SDC = 1$ and $WCDE \neq 0$ even without direct discrimination. In such cases, no algorithm can identify the true WCDE. The identifiability of any direct effect measure is fundamentally limited by the observability of backdoor and frontdoor paths. Users should exercise caution when interpreting results.

3.1 A Graphical Criterion for the Weighted CDE

Definition 8 (Graphical criterion for identifying the WCDE). Under the causal partition taxonomy defined in

Maasch et al. (2024), we define the set \mathbf{A}_{DE} that contains all parents of the outcome:

$$\mathbf{A}_{DE} := \mathbf{Z}_{1 \in pa(Y)} \cup \mathbf{Z}_{3 \in pa(Y)} \cup \mathbf{Z}_{4 \in pa(Y)}. \quad (5)$$

Theorem 2 (\mathbf{A}_{DE} is a VAS for the WCDE). \mathbf{A}_{DE} is a valid adjustment set for the WCDE. It satisfies the identification conditions in Definition 5 by blocking (1) all backdoor paths of $\{X, Y\}$, (2) all backdoor paths of $\{M, Y\}$, and (3) all frontdoor paths of $\{X, Y\}$.

Intuition. \mathbf{A}_{DE} contains exactly all the parents of Y : confounders of $\{X, Y\}$ adjacent to Y ($\mathbf{Z}_{1 \in pa(Y)}$), mediators of $\{X, Y\}$ adjacent to Y ($\mathbf{Z}_{3 \in pa(Y)}$), and all parents of Y that are marginally independent of X ($\mathbf{Z}_{4 \in pa(Y)}$). Thus, at least one member of every backdoor and frontdoor path is in \mathbf{A}_{DE} . This provides conditional d -separation of X and Y if and only if there is no edge $X \rightarrow Y$. Proof is in Appendix B.

Remark 2 (The role of \mathbf{Z}_4). Note that \mathbf{Z}_3 and Y can be confounded by \mathbf{Z}_1 , \mathbf{Z}_3 , or \mathbf{Z}_4 (Figure B.1). Including $\mathbf{Z}_{4 \in pa(Y)}$ in \mathbf{A}_{DE} helps guarantee the identifiability of WCDE without requiring exact knowledge of confounding for \mathbf{Z}_3 and Y . Adjusting for \mathbf{Z}_4 has been shown to reduce estimate variance in propensity score models (Brookhart et al. 2006), and convention dictates that adjustment should minimally constrain the exposure and maximally constrain the outcome (Runge 2021). Thus, there may be statistical benefits to including $\mathbf{Z}_{4 \in pa(Y)}$ in \mathbf{A}_{DE} , though we do not formally explore this.

Remark 3 (Statistical efficiency and interpretability). Given A1 and A2, adjusting for all \mathbf{Z} would not induce bias in WCDE. However, this is likely to constitute *unnecessary adjustment* and is generally not advised, as it can lead to variance inflation in the final estimate (Schisterman, Cole, and Platt 2009). For statistical efficiency, minimal or optimal adjustment is preferred (Brookhart et al. 2006; Rotnitzky and Smeucler 2020; Runge 2021). While \mathbf{A}_{DE} may not be minimal or optimal in all cases, adjusting only for the parents of Y is a simple heuristic to avoid unnecessary adjustment. Unnecessary adjustment also diminishes the *interpretability* of adjustment sets by allowing extraneous variables, undermining actionable fairness conclusions. Appendix C.5 empirically illustrates the pitfalls of unnecessary adjustment.

4 Related Works

Discovery for CFA Few works in causal discovery have centered on fairness objectives (Binkytė et al. 2023). These include learning Suppes-Bayes causal networks with maximum likelihood estimation (Bonchi et al. 2017) and applying PC Algorithm (Zhang, Wu, and Wu 2017). To our knowledge, this work presents the first *local* causal discovery method that is specifically tailored for CFA.

Local Discovery of Direct Causes Learning the direct causes of a target has primarily garnered interest in causal feature selection. Soleymani et al. (2022) adopt Assumption A1 to show that double machine learning (Chernozhukov et al. 2018) can identify the parents of a target without assuming faithfulness or acyclicity. Various Markov blanket (MB) learners have been proposed, though many cannot distinguish parents from children and/or spouses (Yu et al.

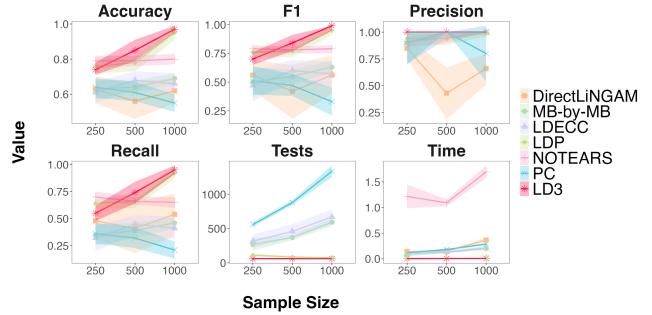


Figure 3: Baseline results for parent discovery in SANGIOVESE. Independence test count (Tests) is reported for constraint-based methods. Time is in seconds. Shaded regions denote 95% confidence intervals over ten replicates.

2020). MB-by-MB (Wang et al. 2014), Causal Markov Blanket (CMB; Gao and Ji 2015), and Local Discovery using Eager Collider Checks (LDECC; Gupta, Childers, and Lipton 2023) are constraint-based methods that differentiate parents and children when unambiguous over the Markov equivalence class (MEC). Like the global algorithm PC (Spirtes et al. 2001), MB-by-MB, CMB, and LDECC have exponential time complexity with respect to variable set size in the worst case. Local Discovery by Partitioning (LDP; Maasch et al. 2024) causally partitions variables around an exposure-outcome pair, using a quadratic number of independence tests with respect to variable set size. Results can be post-processed to identify the outcome’s parents if A1 is imposed.

5 Empirical Validation on Synthetic Data

Baselines Baselines were selected to represent a range of approaches that are available as open-source Python implementations. Local baselines are MB-by-MB (Wang et al. 2014), LDECC (Gupta, Childers, and Lipton 2023), and LDP (Maasch et al. 2024). Global baselines are PC (Spirtes et al. 2001), DirectLiNGAM (Shimizu et al. 2011), and NOTEARS (Zheng et al. 2018). Extended baseline descriptions and post-processing procedures are given in Appendix C.2. Besides LDP, all baselines assume causal sufficiency. PC, MB-by-MB, and LDECC return results in terms of the MEC. DirectLiNGAM assumes an additive noise model. DirectLiNGAM and NOTEARS assume linearity. All experiments used an Apple MacBook (M2 Pro Chip; 12 CPU cores; 16G memory).

Parent Discovery As the SDC and WCDE graphical criterion used in this work require that all parents of the outcome are correctly identified, we evaluated whether LD3 can recover true parent sets. We tested LD3 with an oracle independence test on random exposure-outcome pairs in 90 unique directed acyclic Erdős-Rényi graphs (node counts in $[5 \dots 500]$) (Erdős, Rényi et al. 1960). Parent F1, recall, and precision were 100%. Runtimes and total independence tests as node and edge cardinality scale are shown in Figure C.2.

All baselines were assessed on the SANGIOVESE benchmark from the bnlearn repository (Scutari 2010), a

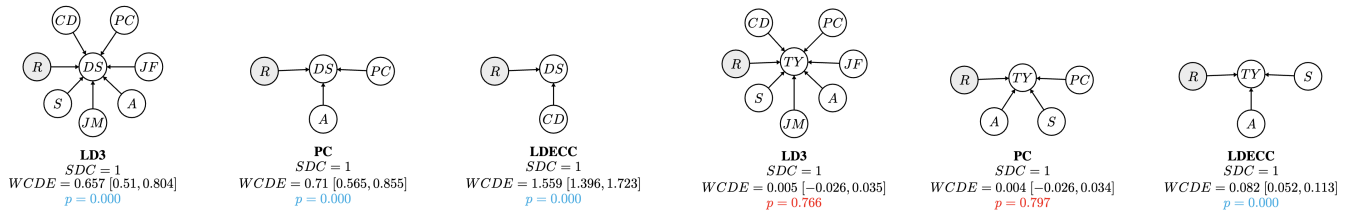


Figure 4: Predicted parent sets, SDC, and WCDE estimates for COMPAS. Exposure is race (R) and outcome is general recidivism risk decile score (DS) or actual two-year recidivism (TY). A = age; CD = charge degree; JF = juvenile felonies; JM = juvenile misdemeanors; PC = priors count; S = sex. WCDE is reported with p -value (p) and 95% confidence intervals in brackets. All methods used χ^2 independence tests ($\alpha = 0.05$). Results for additional significance levels are in Figures D.3–D.5.

linear-Gaussian model of Tuscan Sangiovese grape production (Magrini, Di Blasi, and Stefanini 2017). Ten replicate datasets were sampled at $n = [250, 500, 1000]$. All constraint-based methods used Fisher-z tests ($\alpha = 0.01$). DirectLiNGAM assumes non-Gaussian noise, and was expected to underperform. LD3 was generally most performant across metrics, with LDP performing similarly (Figure 3, Table C.5). NOTEARS was significantly slower than other methods. Comparisons of LD3 to LDECC, LDP, and PC on ASIA (Lauritzen and Spiegelhalter 1988) and SACHS (Sachs et al. 2005) benchmarks are in Tables C.6 and C.8. Runtime comparisons are in Figure C.2 and Tables C.7, C.9.

Weighted CDE Estimation To evaluate SDC and WCDE correctness, we tested LD3 on linear-Gaussian instantiations of an 18-node DAG with an M-structure (i.e., a member of $\mathbf{Z}_{2 \notin de(Y)}$; Ding and Miratrix 2015) and multiple members of \mathbf{Z}_1 , \mathbf{Z}_3 , and \mathbf{Z}_4 (Figure C.1). The WCDE was estimated using linear regression with \mathbf{A}_{DE} as covariates. \mathbf{A}_{DE} F1, precision, and recall and SDC accuracy converged toward 100% as sample size increased. The WCDE converged toward the true direct effect with low variance (Figures C.3, C.4). LD3 can reduce unnecessary adjustment relative to adjusting for all \mathbf{Z} (Schisterman, Cole, and Platt 2009), as illustrated in Appendix C.5. Variance using all \mathbf{Z} was at least $12.6\times$ higher than using \mathbf{A}_{DE} from LD3 for a nonlinear SCM (Table C.2).

6 Real-World Causal Fairness Analyses

We deploy LD3 for two causal fairness settings: (1) racial discrimination in criminal recidivism prediction and (2) sex-based discrimination in healthcare. We compare the results of LD3 to PC and LDECC on the basis of \mathbf{A}_{DE} quality and computational efficiency. Causal discovery used χ^2 independence tests and WCDE estimation used double machine learning (Chernozhukov et al. 2018).⁴ Estimators used random forest classifiers with a 70%/30% train-test split.⁵ We assumed A1 and A2. We assumed that conditioning on confounders for $\{M, Y\}$ that might be descended from X did not open backdoor paths (Petersen et al. 2006; Pearl 2014; Imai 2023). Data preprocessing is described in Appendix D.

⁴<https://econml.azurewebsites.net>

⁵<https://scikit-learn.org>

6.1 Race and COMPAS Recidivism Prediction

Background We assessed the ability of LD3 to facilitate CFA on the COMPAS dataset from ProPublica⁶ (Angwin et al. 2022). Correctional Offender Management Profiling for Alternative Sanctions (COMPAS) is a commercial algorithm for case management and decision support used by the US criminal justice system to assess risk of recidivism (NorthPointe 2015). ProPublica’s landmark exposé on COMPAS found that African Americans are “almost twice as likely as whites to be labeled a higher risk but not actually re-offend” (Table 2).

	White	AA
Labeled higher risk, not reoffender	23.5%	44.9%
Labeled lower risk, reoffender	47.7%	28.0%

Table 2: COMPAS risk assessment in African Americans (AA) vs white Americans (from Angwin et al. 2022).

We examined racial bias in the COMPAS General Recidivism Risk model. Due to data availability, we limited our analyses to the most represented racial groups (black and white). The algorithm’s developer states that the model directly considers prior criminal history and juvenile delinquency, among other factors (NorthPointe 2015, p. 27). Our data contained multiple indicators of criminal history and juvenile delinquency, so these were used to assess the quality of causal discovery in lieu of complete ground truth. We used three significance levels for independence testing ($\alpha = 0.005, 0.01, 0.05$) to assess stability of results (Figures 4, D.3–D.5). We selected 11 features with $n = 6150$ observations (2454 white, 3696 black; see Appendix D). We explored two outcomes: (1) *general recidivism decile score* to probe bias in the COMPAS algorithm, and (2) *actual two-year recidivism*, to examine factors in real outcomes.

Results At all significance levels, results from LD3, PC, and LDECC qualitatively agree that the effects of race on decile score are not fully explained by observed⁷ confounding and mediation (SDC = 1) and that the WCDE is significant ($p = 0.000$). LD3 successfully predicted that juvenile

⁶github.com/propublica/compas-analysis

⁷Note that if A2 was violated, some of the observed effects might be due to unobserved variables. This is unverifiable using ProPublica’s data alone. See Remark 1.

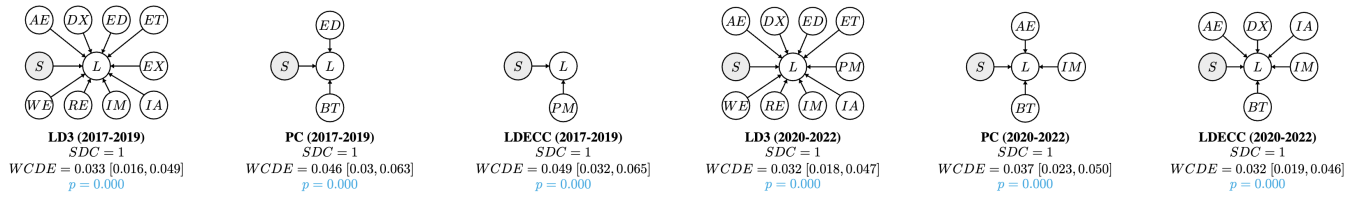


Figure 5: Predicted parent sets, SDC, and WCDE estimates for STAR liver data. Exposure is patient sex (S) and outcome is receiving a liver (L). *AE* = active exception case; *BT* = recipient blood type; *DX* = diagnosis; *ED* = education; *ET* = ethnicity; *EX* = exception type; *IA* = initial age; *IM* = initial MELD; *PM* = payment method; *RE* = region; *WE* = weight. WCDE is reported with p -value (p) and 95% confidence intervals in brackets. All methods used χ^2 independence tests ($\alpha = 0.01$).

delinquency is a parent of decile score at all significance levels, while PC and LDECC never did. Age, priors count, and charge degree were nearly always predicted to be parents across methods and significance levels. For two-year recidivism, LD3 stably predicted that the WCDE of race was not significant ($p = 0.87, 0.68, 0.77$).

In general, results for PC and LDECC were less stable than LD3. Both methods wavered between strong significance ($p = 0.000$) and no significance ($p > 0.4$) for the WCDE of race on two-year recidivism. LDECC parent sets were inconsistent depending on whether they were taken as the intersection or union across graphs in the MEC, requiring additional interpretation by the user. On average, PC and LDECC took $46\times$ longer to run and performed at least $11.7\times$ more tests than LD3 across experiments (Figure D.2).

6.2 Sex and Liver Transplant Allocation

Background We apply LD3 to a real-world case study in the US healthcare system: fairness in liver transplant allocation. Liver transplantation is a critical therapeutic option for patients with end-stage chronic liver disease and acute liver failure. Demand significantly surpasses supply for donor livers (SRTR 2020), and patients are placed on a national waiting list managed by the United Network for Organ Sharing (UNOS). The distribution policy sorts waitlisted patients by multiple criteria, such as medical urgency, compatibility, and location (Latt, Niazi, and Pysopoulos 2022). Several key policy changes have sought to optimize distribution and improve patient outcomes (Papalexopoulos et al. 2023; see Appendix D.2), including the *model for end-stage liver disease* (MELD; Malinchoc et al. 2000). Despite efforts to increase fairness (Kim et al. 2022), it is widely recognized that US organ allocation suffers from disparities on the basis of race, sex, and socioeconomic status (Zhang et al. 2018).

We explored potential sex-based discrimination in liver allocation. Sex-based disparities have been observed as statistical associations (Mathur et al. 2011; Gordon and Ladner 2012; Sarkar et al. 2015,?; Oloruntoba and Moylan 2015; Allen et al. 2018; Nephew and Serper 2021), but have not been explored through a causal lens. We use the National Standard Transplant Analysis and Research (STAR) dataset (OPTN 2024) for adult patients during 2017-2019 ($n = 21, 101$) and 2020-2022 ($n = 22, 807$). See Appendix D.2 for feature selection and summary statistics.

Results Under all experimental settings and time frames, results from LD3 suggest that the effects of sex on receiving a liver are not fully explained by observed confounding and mediation (Figure 5, Table D.2). Causal evidence of direct discrimination is detected (SDC = 1) and corroborated by non-zero WCDE with significant p -values (< 0.005). In all settings, \mathbf{A}_{DE} contains key factors used in the liver distribution policy, including initial MELD, initial age, region, and active exception case (OPTN 2024). Our results are concordant with prior observations that differences in body size and medical condition contribute to sex-based disparities (Nephew et al. 2017), as weight and diagnosis are in \mathbf{A}_{DE} in all settings. Predicted \mathbf{A}_{DE} also indicate potential discrimination with respect to ethnicity, education, and payment method. These socioeconomic factors may warrant further investigation for future policy interventions. These preliminary results are only qualitative indicators, and further analyses should take place.

PC and LDECC qualitatively agree with LD3 on both discrimination metrics (Tables D.3, D.4). However, PC, LDECC, and LD3 had relatively low agreement in terms of \mathbf{A}_{DE} . Adjustment set cardinality was lower (and at times zero) for PC and LDECC. Most settings for PC and LDECC returned \mathbf{A}_{DE} that omitted key expected variables, such as known policy criteria (e.g., initial MELD score, active exception case, and initial age). In Figure 5, we show the most favorable results from PC and LDECC ($\alpha = 0.01$). At both significance levels, PC returned multiple untrustworthy edges (e.g., weight \rightarrow sex, height \rightarrow sex, blood type \rightarrow age, education \rightarrow height, body mass index \rightarrow height), undermining the credibility of results. Likewise, LDECC predicts that the outcome has children, which is known to be untrue. PC performed $479\text{--}1021\times$ more tests and took $2295\text{--}5870\times$ longer to execute than LD3 (Table D.5). LDECC performed $42\text{--}984\times$ more tests and took $197\text{--}5774\times$ longer to run.

7 Conclusion

This work advocates for increased practicality in causal fairness pipelines. We propose a time-efficient and asymptotically correct local discovery method for identifying two qualitative measures of direct discrimination: the SDC and WCDE. We provide a graphical criterion for WCDE identification that limits unnecessary adjustment for statistically efficient and interpretable adjustment sets. For two real-world causal fairness analyses, LD3 returned more stable and plau-

sible predictions with significantly better computational efficiency relative to baselines.

Limitations and Future Directions Future work could extend LD3 to allow for Y with descendants. The assumption that all parents of Y are observed is sufficient but not necessary for CDE identification and could be replaced with a different criterion. LD3 cannot differentiate Z_1 from Z_3 , which would enable analysis of indirect and spurious discrimination. Future work could consider discovery for other fairness estimands, such as the natural effects (Pearl 2014) and path-specific effects (Avin, Shpitser, and Pearl 2005).

References

- Allen, A. M.; Heimbach, J. K.; Larson, J. J.; Mara, K. C.; Kim, W. R.; Kamath, P. S.; and Therneau, T. M. 2018. Reduced access to liver transplantation in women: role of height, MELD exception scores, and renal function underestimation. *Transplantation*, 102(10): 1710–1716.
- Andrews, R. M.; and Didelez, V. 2021. Insights into the cross-world independence assumption of causal mediation analysis. *Epidemiology*, 32(2): 209–219.
- Angwin, J.; Larson, J.; Mattu, S.; and Kirchner, L. 2022. Machine bias. In *Ethics of data and analytics*, 254–264. Auerbach Publications.
- Avin, C.; Shpitser, I.; and Pearl, J. 2005. Identifiability of path-specific effects. In *IJCAI International Joint Conference on Artificial Intelligence*, 357–363.
- Bareinboim, E.; Correa, J. D.; Ibeling, D.; and Icard, T. 2022. On Pearl’s hierarchy and the foundations of causal inference. In *Probabilistic and causal inference: the works of judea pearl*, 507–556. ACM.
- Barocas, S.; and Selbst, A. D. 2016. Big data’s disparate impact. *California Law Review*, 104: 671.
- Binkytė, R.; Makhlof, K.; Pinzón, C.; Zhioua, S.; and Palamidessi, C. 2023. Causal discovery for fairness. In *Workshop on Algorithmic Fairness through the Lens of Causality and Privacy*, 7–22. PMLR.
- Bonchi, F.; Hajian, S.; Mishra, B.; and Ramazzotti, D. 2017. Exposing the probabilistic causal structure of discrimination. *International Journal of Data Science and Analytics*, 3: 1–21.
- Brookhart, M. A.; Schneeweiss, S.; Rothman, K. J.; Glynn, R. J.; Avorn, J.; and Stürmer, T. 2006. Variable Selection for Propensity Score Models. *American Journal of Epidemiology*, 163(12): 1149–1156.
- Cai, H.; Wang, Y.; Jordan, M.; and Song, R. 2023. On learning necessary and sufficient causal graphs. *Advances in Neural Information Processing Systems*, 36.
- Carey, A. N.; and Wu, X. 2022. The causal fairness field guide: Perspectives from social and formal sciences. *Frontiers in big Data*, 5: 892837.
- Cheng, D.; Li, J.; Liu, L.; Zhang, J.; Liu, J.; and Le, T. D. 2022. Local search for efficient causal effect estimation. *IEEE Transactions on Knowledge and Data Engineering*, 1–14.
- Chernozhukov, V.; Chetverikov, D.; Demirer, M.; Duflo, E.; Hansen, C.; Newey, W.; and Robins, J. 2018. Double/debiased machine learning for treatment and structural parameters. *The Econometrics Journal*, 21: C1–C68.
- Chickering, D. M. 2002. Optimal Structure Identification With Greedy Search. *Journal of Machine Learning Research*, 3.
- Chickering, D. M.; Heckerman, D.; and Meek, C. 2004. Large-Sample Learning of Bayesian Networks is NP-Hard. *Journal of Machine Learning Research*, 5: 1287–1330.
- Claassen, T.; Mooij, J. M.; and Heskes, T. 2013. Learning Sparse Causal Models is not NP-hard. *Proceedings of the Twenty-Ninth Conference on Uncertainty in Artificial Intelligence (UAI2013)*.
- Conati, C.; Gertner, A. S.; VanLehn, K.; and Druzdzel, M. J. 1997. On-line student modeling for coached problem solving using Bayesian networks. In *User Modeling: Proceedings of the Sixth International Conference UM97 Chia Laguna, Sardinia, Italy June 2–5 1997*, 231–242. Springer.
- Corbett-Davies, S.; Gaebler, J. D.; Nilforoshan, H.; Shroff, R.; and Goel, S. 2023. The measure and mismeasure of fairness. *The Journal of Machine Learning Research*, 24(1): 14730–14846.
- Dai, H.; Ng, I.; Zheng, Y.; Gao, Z.; and Zhang, K. 2024. Local Causal Discovery with Linear non-Gaussian Cyclic Models. In *International Conference on Artificial Intelligence and Statistics*, 154–162. PMLR.
- Ding, P.; and Miratrix, L. W. 2015. To adjust or not to adjust? Sensitivity analysis of M-bias and butterfly-bias. *Journal of Causal Inference*, 3(1): 41–57.
- Erdős, P.; Rényi, A.; et al. 1960. On the evolution of random graphs. *Publ. math. inst. hung. acad. sci.*, 5(1): 17–60.
- Gao, T.; and Ji, Q. 2015. Local Causal Discovery of Direct Causes and Effects. In Cortes, C.; Lawrence, N.; Lee, D.; Sugiyama, M.; and Garnett, R., eds., *Advances in Neural Information Processing Systems*, volume 28. Curran Associates, Inc.
- Gordon, E. J.; and Ladner, D. P. 2012. Gender inequities pervade organ transplantation access. *Transplantation*, 94(5): 447–448.
- Gretton, A.; Bousquet, O.; Smola, A.; and Schölkopf, B. 2005. Measuring statistical dependence with Hilbert-Schmidt norms. In *International conference on algorithmic learning theory*, 63–77. Springer.
- Gretton, A.; Fukumizu, K.; Teo, C.; Song, L.; Schölkopf, B.; and Smola, A. 2007. A kernel statistical test of independence. *Advances in neural information processing systems*, 20.
- Guo, F. R.; Lundborg, A. R.; and Zhao, Q. 2022. Confounder Selection: Objectives and Approaches. ArXiv:2208.13871 [math, stat].
- Gupta, S.; Childers, D.; and Lipton, Z. C. 2023. Local Causal Discovery for Estimating Causal Effects. In *Proceedings of the 2nd Conference on Causal Learning and Reasoning (CLear)*. arXiv. ArXiv:2302.08070 [cs, stat].

- Hernán, M. A.; and Robins, J. M. 2006. Instruments for Causal Inference: An Epidemiologist's Dream? *Epidemiology*, 17(4): 360–372.
- Imai, K. 2023. Lecture 09-2: Identification of Indirect Effects. <https://www.youtube.com/watch?v=1WBXsAiU-dk>. "Accessed May 2024".
- Imai, K.; Keele, L.; and Tingley, D. 2010. A general approach to causal mediation analysis. *Psychological methods*, 15(4): 309.
- Imai, K.; Keele, L.; and Yamamoto, T. 2010. Identification, Inference and Sensitivity Analysis for Causal Mediation Effects. *Statistical Science*, 25(1).
- Kalisch, M.; and Bühlman, P. 2007. Estimating high-dimensional directed acyclic graphs with the PC-algorithm. *Journal of Machine Learning Research*, 8(3).
- Kilbertus, N.; Rojas Carulla, M.; Parascandolo, G.; Hardt, M.; Janzing, D.; and Schölkopf, B. 2017. Avoiding discrimination through causal reasoning. *Advances in neural information processing systems*, 30.
- Kim, I. K.; Martins, P. N.; Pavlakis, M.; Eneanya, N. D.; and Patzer, R. E. 2022. Past and Present Policy Efforts in Achieving Racial Equity in Kidney Transplantation. *Current Transplantation Reports*, 9(2): 114–118.
- Kim, W. R.; Mannalithara, A.; Heimbach, J. K.; Kamath, P. S.; Asrani, S. K.; Biggins, S. W.; Wood, N. L.; Gentry, S. E.; and Kwong, A. J. 2021. MELD 3.0: the model for end-stage liver disease updated for the modern era. *Gastroenterology*, 161(6): 1887–1895.
- Latt, N. L.; Niazi, M.; and Prysopoulos, N. T. 2022. Liver transplant allocation policies and outcomes in United States: A comprehensive review. *World Journal of Methodology*, 12(1): 32.
- Lauritzen, S. L. 1988. Local computations with probabilities on graphical structures and their application to expert systems (with discussion). *J. Roy. Statist., Soc., B*, 50(2): 251–263.
- Lauritzen, S. L.; and Spiegelhalter, D. J. 1988. Local Computations with Probabilities on Graphical Structures and Their Application to Expert Systems. *Journal of the Royal Statistical Society: Series B (Methodological)*, 50(2): 157–194.
- Lousdal, M. L. 2018. An introduction to instrumental variable assumptions, validation and estimation. *Emerging Themes in Epidemiology*, 15(1): 1.
- Maasch, J.; Pan, W.; Gupta, S.; Kuleshov, V.; Gan, K.; and Wang, F. 2024. Local Discovery by Partitioning: Polynomial-Time Causal Discovery Around Exposure-Outcome Pairs. In *Proceedings of the 40th Conference on Uncertainty in Artificial Intelligence*.
- Maathuis, M. H.; and Colombo, D. 2015. A generalized back-door criterion. *The Annals of Statistics*, 43(3).
- Magrini, A.; Di Blasi, S.; and Stefanini, F. M. 2017. A conditional linear Gaussian network to assess the impact of several agronomic settings on the quality of Tuscan Sangiovese grapes. *Biometrical Letters*, 54(1): 25–42.
- Makhlouf, K.; Zhioua, S.; and Palamidessi, C. 2020. Survey on causal-based machine learning fairness notions. *arXiv preprint arXiv:2010.09553*.
- Malinchoc, M.; Kamath, P. S.; Gordon, F. D.; Peine, C. J.; Rank, J.; and Ter Borg, P. C. 2000. A model to predict poor survival in patients undergoing transjugular intrahepatic portosystemic shunts. *Hepatology*, 31(4): 864–871.
- Mathur, A. K.; Schaubel, D. E.; Gong, Q.; Guidinger, M. K.; and Merion, R. M. 2011. Sex-based disparities in liver transplant rates in the United States. *American Journal of Transplantation*, 11(7): 1435–1443.
- Montagna, F.; Noceti, N.; Rosasco, L.; Zhang, K.; and Locatello, F. 2023. Causal discovery with score matching on additive models with arbitrary noise. In *Conference on Causal Learning and Reasoning*, 726–751. PMLR.
- Nephew, L. D.; Goldberg, D. S.; Lewis, J. D.; Abt, P.; Bryan, M.; and Forde, K. A. 2017. Exception points and body size contribute to gender disparity in liver transplantation. *Clinical gastroenterology and hepatology*, 15(8): 1286–1293.
- Nephew, L. D.; and Serper, M. 2021. Racial, gender, and socioeconomic disparities in liver transplantation. *Liver Transplantation*, 27(6): 900–912.
- NorthPointe. 2015. Practitioner's Guide to COMPAS Core.
- Oloruntoba, O. O.; and Moylan, C. A. 2015. Gender-based disparities in access to and outcomes of liver transplantation. *World journal of hepatology*, 7(3): 460.
- OPTN. 2024. Data Request Instructions. Accessed: 2024-05-20.
- Papalexopoulos, T.; Alcorn, J.; Bertsimas, D.; Goff, R.; Stewart, D.; and Trichakis, N. 2023. Reshaping national organ allocation policy. *Operations Research*.
- Pearl, J. 1995. Causal diagrams for empirical research. *Biometrika*, 82(4): 669–688.
- Pearl, J. 2001. Direct and Indirect Effects. In *Proceedings of the Seventeenth Conference on Uncertainty in Artificial Intelligence*.
- Pearl, J. 2012a. The Causal Mediation Formula—A Guide to the Assessment of Pathways and Mechanisms. *Prevention Science*, 13(4): 426–436.
- Pearl, J. 2012b. The mediation formula: A guide to the assessment of causal pathways in nonlinear models. *Causality: Statistical perspectives and applications*, 151–179.
- Pearl, J. 2014. Interpretation and identification of causal mediation. *Psychological Methods*, 19(4): 459–481.
- Perkovic, E.; Textor, J.; Kalisch, M.; and Maathuis, M. H. 2015. A Complete Generalized Adjustment Criterion. *Proceedings of the Thirty-First Conference of Uncertainty in Artificial Intelligence (UAI)*, 682–691.
- Petersen, A. H.; Ekstrøm, C. T.; Spirtes, P.; and Osler, M. 2023. Constructing Causal Life-Course Models: Comparative Study of Data-Driven and Theory-Driven Approaches. *American Journal of Epidemiology*, 192(11): 1917–1927.
- Petersen, M. L.; Sinisi, S. E.; and Van Der Laan, M. J. 2006. Estimation of Direct Causal Effects. *Epidemiology*, 17(3): 276–284.

- Plečko, D.; and Bareinboim, E. 2023. Causal Fairness for Outcome Control. In *Proceedings of the 37th Conference on Neural Information Processing Systems (NeurIPS 2023)*.
- Plečko, D.; and Bareinboim, E. 2024. Causal Fairness Analysis: A Causal Toolkit for Fair Machine Learning. *Foundations and Trends® in Machine Learning*, 17(3): 304–589.
- Rotnitzky, A.; and Smucler, E. 2020. Efficient adjustment sets for population average causal treatment effect estimation in graphical models. *Journal of Machine Learning Research*, 21(188): 1–86.
- Runge, J. 2018. Conditional independence testing based on a nearest-neighbor estimator of conditional mutual information. In *Proceedings of the 21st International Conference on Artificial Intelligence and Statistics (AISTATS)*. Lanzarote, Spain.
- Runge, J. 2021. Necessary and sufficient graphical conditions for optimal adjustment sets in causal graphical models with hidden variables. *Proceedings of the 35th Conference on Neural Information Processing Systems*.
- Sachs, K.; Perez, O.; Pe’er, D.; Lauffenburger, D. A.; and Nolan, G. P. 2005. Causal protein-signaling networks derived from multiparameter single-cell data. *Science*, 308(5721): 523–529.
- Sarkar, M.; Watt, K. D.; Terrault, N.; and Berenguer, M. 2015. Outcomes in liver transplantation: does sex matter? *Journal of hepatology*, 62(4): 946–955.
- Schäfer, J.; and Strimmer, K. 2005. A shrinkage approach to large-scale covariance matrix estimation and implications for functional genomics. *Statistical applications in genetics and molecular biology*, 4(1).
- Schisterman, E. F.; Cole, S. R.; and Platt, R. W. 2009. Over-adjustment Bias and Unnecessary Adjustment in Epidemiologic Studies. *Epidemiology*, 20(4): 488–495.
- Scutari, M. 2010. Learning Bayesian networks with the bnlearn R Package. *Journal of Statistical Software*, 35(3).
- Shah, A.; Shanmugam, K.; and Ahuja, K. 2022. Finding Valid Adjustments under Non-ignorability with Minimal DAG Knowledge. ArXiv:2106.11560 [cs].
- Shah, A.; Shanmugam, K.; and Kocaoglu, M. 2024. Front-door Adjustment Beyond Markov Equivalence with Limited Graph Knowledge. *Advances in Neural Information Processing Systems*, 36.
- Shen, X.; Ma, S.; Vemuri, P.; Simon, G.; and The Alzheimer’s Disease neuroimaging initiative. 2020. Challenges and Opportunities with Causal Discovery Algorithms: Application to Alzheimer’s Pathophysiology. *Scientific Reports*, 10(2975).
- Shimizu, S.; Inazumi, T.; Sogawa, Y.; Hyvarinen, A.; Kawahara, Y.; Washio, T.; Hoyer, P. O.; Bollen, K.; and Hoyer, P. 2011. DirectLiNGAM: A direct method for learning a linear non-Gaussian structural equation model. *Journal of Machine Learning Research-JMLR*, 12(Apr): 1225–1248.
- Shpitser, I.; and Pearl, J. 2006. Identification of Conditional Interventional Distributions. In *Proceedings of the Twenty-Second Conference on Uncertainty in Artificial Intelligence*.
- Shpitser, I.; and VanderWeele, T. J. 2011. A Complete Graphical Criterion for the Adjustment Formula in Mediation Analysis. *The International Journal of Biostatistics*, 7(1): 1–24.
- Soleymani, A.; Raj, A.; Bauer, S.; Schölkopf, B.; and Besserve, M. 2022. Causal Feature Selection via Orthogonal Search. *Transactions on Machine Learning Research*. ArXiv:2007.02938 [cs, math, stat].
- Spirtes, P. 2001. An Anytime Algorithm for Causal Inference. In *Proceedings of the Eighth International Workshop on Artificial Intelligence and Statistics*, volume R3, 278–285. PMLR.
- Spirtes, P.; Glymour, C.; and Scheines, R. 2001. *Causation, prediction, and search*. MIT press.
- SRTR. 2020. OPTN/SRTR 2020 Annual Data Report: Liver. Accessed: 2024-05-20.
- Starke, C.; Baleis, J.; Keller, B.; and Marcinkowski, F. 2022. Fairness perceptions of algorithmic decision-making: A systematic review of the empirical literature. *Big Data & Society*, 9(2): 20539517221115189.
- Tsamardinos, I.; Brown, L. E.; and Aliferis, C. F. 2006. The max-min hill-climbing Bayesian network structure learning algorithm. *Machine Learning*, 65(1): 31–78.
- UNOS. 2015. The policy change of adding serum sodium to MELD score calculation. Accessed: May 2024.
- UNOS. 2020. Liver and intestinal organ distribution based on acuity circles implemented Feb. 4. Accessed: May 2024.
- UNOS. 2022. Improving Liver Allocation: MELD, PELD, Status 1A, Status 1B. Accessed: May 2024.
- Vanderweele, T. J. 2011. Controlled Direct and Mediated Effects: Definition, Identification and Bounds. *Scandinavian Journal of Statistics*, 38(3): 551–563.
- VanderWeele, T. J. 2013. Policy-relevant proportions for direct effects. *Epidemiology*, 24(1): 175–176.
- VanderWeele, T. J. 2019. Principles of confounder selection. *European Journal of Epidemiology*, 34(3): 211–219.
- VanderWeele, T. J.; and Shpitser, I. 2013. On the definition of a confounder. *The Annals of Statistics*, 41(1).
- Vansteelandt, S. 2009. Estimating direct effects in cohort and case-control studies. *Epidemiology*, 20(6): 851–860.
- Verma, S.; and Rubin, J. 2018. Fairness definitions explained. In *Proceedings of the international workshop on software fairness*, 1–7.
- Wald, C.; Russo, M. W.; Heimbach, J. K.; Hussain, H. K.; Pomfret, E. A.; and Bruix, J. 2013. New OPTN/UNOS policy for liver transplant allocation: standardization of liver imaging, diagnosis, classification, and reporting of hepatocellular carcinoma.
- Wang, C.; Zhou, Y.; Zhao, Q.; and Geng, Z. 2014. Discovering and orienting the edges connected to a target variable in a DAG via a sequential local learning approach. *Computational Statistics & Data Analysis*, 77: 252–266.
- Yu, K.; Guo, X.; Liu, L.; Li, J.; Wang, H.; Ling, Z.; and Wu, X. 2020. Causality-based feature selection: Methods and evaluations. *ACM Computing Surveys (CSUR)*, 53(5): 1–36.

- Yu, K.; Guo, X.; Liu, L.; Li, J.; Wang, H.; Ling, Z.; and Wu, X. 2021. Causality-based Feature Selection: Methods and Evaluations. *ACM Computing Surveys*, 53(5): 1–36.
- Yu, K.; Liu, L.; and Li, J. 2021. A Unified View of Causal and Non-causal Feature Selection. *ACM Transactions on Knowledge Discovery from Data*, 15(4): 1–46.
- Zhang, J.; and Bareinboim, E. 2018. Fairness in Decision-Making — The Causal Explanation Formula. *Proceedings of the AAAI Conference on Artificial Intelligence*, 32(1).
- Zhang, K.; Peters, J.; Janzing, D.; and Scholkopf, B. 2011. Kernel-based Conditional Independence Test and Application in Causal Discovery. *Proceedings of the Twenty-Seventh Conference on Uncertainty in Artificial Intelligence*.
- Zhang, L.; Wu, Y.; and Wu, X. 2017. A causal framework for discovering and removing direct and indirect discrimination. In *Proceedings of the 26th International Joint Conference on Artificial Intelligence*, 3929–3935.
- Zhang, X.; Melanson, T. A.; Plantinga, L. C.; Basu, M.; Pastan, S. O.; Mohan, S.; Howard, D. H.; Hockenberry, J. M.; Garber, M. D.; and Patzer, R. E. 2018. Racial/ethnic disparities in waitlisting for deceased donor kidney transplantation 1 year after implementation of the new national kidney allocation system. *American Journal of Transplantation*, 18(8): 1936–1946.
- Zheng, X.; Aragam, B.; Ravikumar, P. K.; and Xing, E. P. 2018. Dags with no tears: Continuous optimization for structure learning. *Advances in neural information processing systems*, 31.

Ethical Statement

Matters of unfairness and direct discrimination have real, profound impacts on human well-being and are often challenging to detect in real-world retrospective data. Researchers who deploy automated methods like LD3 should be prudent in interpreting and publicly communicating the statistical significance and uncertainty of their findings, whether evidence for or against discrimination is found.

Appendix

A Further Discussion on Direct Effect Estimation

A.1 Comparison of Direct Effect Measures

Here we explore the differences and similarities between the CDE and alternative direct effect measures, and provide justification for our use of the CDE in this work.

Multiple measures of direct effects have been proposed, including the CDE, the NDE (Pearl 2001), and the Ctf-DE (Zhang and Bareinboim 2018). The CDE is an interventional quantity, while the NDE and Ctf-DE are counterfactual quantities. Relative to the CDE, the NDE and Ctf-DE require additional assumptions on the data generating process and more prior structural knowledge for identifiability (Vanderweele 2011). The NDE and Ctf-DE also correspond less directly to real-world interventions, limiting their utility in policy evaluation (Vanderweele 2011; Vanderweele 2013). As previously noted, the CDE, NDE, and Ctf-DE are all zero when there is no edge $X \rightarrow Y$. As detection of this edge is the primary objective of this work, we advocate for the simpler estimand. Though the NDE and Ctf-DE have useful properties for certain forms of analysis, we restrict our attention to the WCDE for these reasons.

Alternative Direct Effect Measures We elaborate on the comparison between the CDE and its most popular counterpart, the NDE (of which the Ctf-DE is an extension). The CDE measures the expected change in outcome as the exposure changes given covariates \mathbf{S} , when mediators \mathbf{M} are uniformly fixed to \mathbf{m} : a *constant value over the population*, as simulated by conditioning on \mathbf{M} (Pearl 2012a). We express the CDE as

$$\text{CDE}(\mathbf{m}) := \mathbb{E}[Y_{x,\mathbf{m}} - Y_{x^*,\mathbf{m}}] \quad (6)$$

$$= \mathbb{E}[Y|do(X = x, \mathbf{M} = \mathbf{m})] - \mathbb{E}[Y|do(X = x^*, \mathbf{M} = \mathbf{m})] \quad (7)$$

$$= \sum_{\mathbf{s}} [\mathbb{E}[Y|x, \mathbf{s}, \mathbf{m}] - \mathbb{E}[Y|x^*, \mathbf{s}, \mathbf{m}]] P(\mathbf{s}). \quad (8)$$

To obtain a unique estimate irrespective of potential interactions between X and \mathbf{M} , we marginalize over the mediator values:

$$\text{WCDE} := \sum_{\mathbf{m}} \sum_{\mathbf{s}} [\mathbb{E}[Y|x, \mathbf{s}, \mathbf{m}] - \mathbb{E}[Y|x^*, \mathbf{s}, \mathbf{m}]] P(\mathbf{m}) P(\mathbf{s}). \quad (9)$$

In contrast, the NDE measures the expected change in outcome as the exposure changes, with mediators fixed at the values that they would have been *per individual* prior to this change in exposure. The NDE captures the portion of the total causal effect that would be transmitted to the outcome if the mediators did not respond to changes in the exposure.

Definition A.1 (Average NDE, Pearl 2014). For values of the exposure x and x^* , values \mathbf{s} of covariates \mathbf{S} , and values \mathbf{m} of mediators \mathbf{M} , the average NDE is

$$\text{NDE}(x, x^*; Y) = \mathbb{E}[Y_{x, \mathbf{M}_x^*} - Y_{x^*, \mathbf{M}_x^*}]. \quad (10)$$

The NDE requires probabilities of nested counterfactuals and a cross-world counterfactual assumption (Shpitser and Vanderweele 2011; Pearl 2012b, 2014; Andrews and Didelez 2021). Nevertheless, Pearl (2001) showed that the NDE can be expressed with *do*-notation and reduced to a *do*-free expression by valid covariate adjustment, allowing for identification and estimation (Pearl 2012b). The average NDE in Markovian models is identifiable from observational data per Corollary 2 in Pearl (2001), allowing counterfactual expressions to be replaced by probabilistic estimands:

$$\text{NDE}(x, x^*; Y) = \sum_{\mathbf{m}} \sum_{\mathbf{s}} [\mathbb{E}[Y|x, \mathbf{s}, \mathbf{m}] - \mathbb{E}[Y|x^*, \mathbf{s}, \mathbf{m}]] P(\mathbf{m}|x^*, \mathbf{s}) P(\mathbf{s}). \quad (11)$$

Note that the WCDE and NDE differ only by the way that we weigh the CDE: for the WCDE, we weigh by $P(\mathbf{m})$, and for the NDE, we weigh by $P(\mathbf{m}|x^*, \mathbf{s})$. This stems from the fact that the CDE is a function of interventional distributions, while the NDE is a counterfactual quantity. Meanwhile, the Ctf-DE measures NDEs conditioned on the subpopulation $X = x$ (Zhang and Bareinboim 2018).

Total Effect Decomposition Unlike the NDE, the CDE does not admit a valid decomposition of the total causal effect into direct and indirect effects for the general nonparametric setting (Pearl 2001). Conversely, the total effect is always equal to the difference of the NDE and the reverse transition of the natural indirect effect (NIE), even in the presence of nonlinearities and exposure-mediator interactions (Pearl 2014). However, in the absence of exposure-mediator interaction, the CDE and NDE are equivalent and the CDE can be used for total effect decomposition (Vanderweele 2011). Guaranteed total effect decomposability is a primary reason that the natural effects are employed in CFA (Plečko and Bareinboim 2024). However, when qualitative indicators of direct discrimination are all that is needed, it suffices to estimate the CDE (Zhang and Bareinboim 2018).

Identifiability Assumptions For our current objectives, we favor the WCDE as a metric because it requires fewer assumptions over the data generating process and requires less prior structural knowledge than the NDE (Vanderweele 2011). For example, the NDE requires that no confounder for $\{M, Y\}$ is descended from X (Pearl 2014), as the same covariates that deconfound $\{M, Y\}$ must also be used to identify the counterfactual quantity $P(\mathbf{m}|x^*, s)$. As explained in Appendix C of Pearl (2014), if this covariate set contains a variable that is descended from the exposure, $P(\mathbf{m}|x^*, s)$ is not identifiable even under random treatment assignment. The absence of confounders of this form is challenging to verify (Vanderweele 2011), and may be unrealistic in real-world data. This limits the range of structures for which unbiased NDE estimates can be obtained. Additionally, the identifiability of the NDE requires that \mathbf{S} also deconfounds $\{X, M\}$, adding an extra burden of graphical knowledge. See Andrews and Didelez (2021) for a discussion of the cross-world counterfactual assumption in NDE identification.

Adjusting for confounders for $\{M, Y\}$ that are descended from the exposure can also induce bias in CDE estimation. However, unlike for the NDE, this bias is addressable when given an appropriate estimator (Petersen, Sinisi, and Van Der Laan 2006; Pearl 2014; Imai 2023). Therefore, the presence or absence of such variables is something that can be assumed at the estimation stage at the discretion of the user. Note that this does not impact the behavior of LD3.

A.2 Graphical Criteria for Direct Effect Identification

Sufficient and necessary conditions for identification vary by estimand, but generally require covariate adjustment (VanderWeele 2019). Formal graphical rules can allow the VAS to be read directly from causal structures, even in the presence of latent confounding (Perkovic et al. 2015; Maathuis and Colombo 2015; Runge 2021). Graphical criteria for valid adjustment have been proposed for diverse causal quantities (e.g., Pearl’s backdoor criterion for total effect estimation; Pearl 1995). Often, multiple valid criteria exist per estimand. These vary in the amount of prior structural knowledge required, and criteria that require less knowledge are easier to implement in practice (VanderWeele and Shpitser 2013; Guo, Lundborg, and Zhao 2022).

Several graphical criteria have been proposed for the identification of direct effects and related quantities. Shpitser and Pearl (2006) present a complete graphical criterion for conditional interventional distributions. Pearl (2001) defines a graphical criterion for identifying the NDE from observational data (Corollary 1). Discussion, debate, and confusion around the sufficient and necessary conditions for NDE identification have inspired a flurry of papers (Imai, Keele, and Yamamoto 2010; Imai, Keele, and Tingley 2010), as summarized in Pearl (2014). Shpitser and VanderWeele (2011) present a complete graphical criterion for the NDE that reconciles some debate, showing where common criteria coincide (Gao and Ji 2015).

Graphical criteria for direct effect estimation are often challenging for practitioners to implement (Shpitser and VanderWeele 2011). To increase the practicality of covariate adjustment in complex and low-knowledge domains, we advocate for the development of graphical criteria that are (1) relatively intuitive and practical to implement in applied research, and (2) are satisfied by knowledge that can be reliably learned through data-driven methods. Thus, we apply the causal partition taxonomy of Maasch et al. (2024) to provide local graphical intuition for fast and practical adjustment set discovery.

B Proofs

B.1 Correctness of Algorithm 1

Proof. We show that each set of tests is correct when all stated assumptions are met.

- \mathbf{Z}_8 (Line 3): As proven in (Maasch et al. 2024), the independence relations tested in Line 3 uniquely define partition \mathbf{Z}_8 and are therefore an asymptotically correct test for identifying this partition, and this partition only.
- $\mathbf{Z}_{5,7}$ (Line 4): As proven in (Maasch et al. 2024), the independence relations tested in Line 4 define partition \mathbf{Z}_7 in all structures and \mathbf{Z}_5 in structures for which $|\mathbf{Z}_1| = 0$ (i.e., no confounders, latent nor observed, exist for X and Y). Therefore, this test is asymptotically guaranteed to return all \mathbf{Z}_7 for arbitrary structures, and all \mathbf{Z}_5 if \mathbf{Z}_1 is the empty set.
- \mathbf{Z}_4 (Line 5): As proven in (Maasch et al. 2024), the independence relations tested in Line 5 uniquely define partition \mathbf{Z}_4 and are therefore an asymptotically correct test for identifying this partition, and this partition only.
- $\mathbf{Z}_{1 \in pa(Y)} \cup \mathbf{Z}_{3 \in pa(Y)}$ (Line 8): At this stage, the only partitions remaining under consideration are \mathbf{Z}_1 , $\mathbf{Z}_{2 \notin de(Y)}$, \mathbf{Z}_3 , and \mathbf{Z}_5 (assuming that \mathbf{Z}_1 is not the empty set). By definition, no \mathbf{Z}_5 will ever be adjacent to Y , as this partition cannot share a causal path to Y that is not mediated by X (Hernán and Robins 2006; Lousdal 2018; Maasch et al. 2024). All $\mathbf{Z}_{2 \notin de(Y)}$ are descended from \mathbf{Z}_1 , \mathbf{Z}_3 , and/or \mathbf{Z}_4 (i.e., any partition that can enter into Y), but not from Y itself. Thus, all \mathbf{Z}_2 and \mathbf{Z}_5 will be eliminated by eliminating variables not adjacent to Y given $X \cup \mathbf{Z}_4 \cup \{\mathbf{Z}' \setminus Z\}$. This test will also result in the elimination of \mathbf{Z}_1 and \mathbf{Z}_3 that are not adjacent to Y , including proxy confounders and proxy mediators as defined in Maasch et al. (2024).
- $\mathbf{Z}_{4 \in pa(Y)}$ (Line 10): Any intervening node on the causal path from \mathbf{Z}_4 to Y ($\mathbf{Z}_4 \rightarrow \dots \rightarrow Y$) must also belong to a partition that can enter into Y ($\dots \rightarrow Y$). By definition, this is strictly \mathbf{Z}_1 , \mathbf{Z}_3 , and \mathbf{Z}_4 . Therefore, to obtain d -separation between Y and any member of \mathbf{Z}_4 that is *not* adjacent to Y , a correct conditioning set will contain X and members of \mathbf{Z}_1 , \mathbf{Z}_3 and \mathbf{Z}_4 . Conditioning on X is essential, as the remaining conditioning set can open noncausal paths between \mathbf{Z}_4 and Y . It is

therefore sufficient to condition on all \mathbf{Z}_1 and \mathbf{Z}_3 that are already known to be adjacent to Y , unioned with X and all known \mathbf{Z}_4 . Any variable that is marginally dependent on Y given this conditioning set is a member of \mathbf{Z}_4 that is adjacent to Y .

- \mathbf{A}_{DE} (Line 11): By definition of \mathbf{A}_{DE} .
- SDC (Line 12): By definition of the SDC (Definition 3), $SDC = \mathbf{1}(X \in pa(Y))$. If X is not a parent of Y , it will always be d -separable from Y when all their confounding and mediating paths are blocked. If X is a parent of Y , X and Y will be always conditionally *dependent* given any conditioning set. Therefore, the SDC will evaluate to 0 if and only if $X \perp\!\!\!\perp Y | \mathbf{Z}_{1 \in pa(Y)} \cup \mathbf{Z}_{3 \in pa(Y)}$.

□

B.2 Proof of Theorem 1

We show that latent variables that are not parents of Y do not impact the asymptotic guarantees of Algorithm 1.

Proof. Maasch et al. (2024) have shown previously that the marginal and conditional independence tests used to identify \mathbf{Z}_4 and \mathbf{Z}_8 are not affected by latent variables. Intuition for this follows from the fact that these tests only require knowledge of $\{X, Y\}$ and the candidate variable Z . In Algorithm 1, the test for $\mathbf{Z}_{5,7}$ also relies only on knowledge of X, Y , and Z , and is therefore correct in the presence of latent variables. As we do not require identification of \mathbf{Z}_5 itself for downstream results, this test suffices. Otherwise, latent variables could pose identifiability problems for \mathbf{Z}_5 , as in prior works (Maasch et al. 2024). A2 alone is sufficient to ensure d -separation between Y and its non-parents at Lines 8 and 10, guaranteeing identification of the true parents of Y in $\mathbf{Z}_1, \mathbf{Z}_3$, and \mathbf{Z}_4 . Therefore, latent variables that are not parents of Y have no impact on Algorithm 1. □

B.3 Proof of Theorem 2

Proof. This theorem claims that $\mathbf{A}_{DE} := \mathbf{Z}_{1 \in pa(Y)} \cup \mathbf{Z}_{3 \in pa(Y)} \cup \mathbf{Z}_{4 \in pa(Y)}$ is a VAS for WCDE identification. Per the identifiability conditions of the WCDE (Definition 5), a VAS must block all backdoor paths for $\{X, Y\}$ and $\{M, Y\}$. As shown in Pearl (2001), knowledge of all mediators for $\{X, Y\}$ that are parents of Y is sufficient for identifying the CDE (i.e., knowledge of every mediator in the full causal graph is unnecessary). Thus, we show that adjusting for \mathbf{A}_{DE} (1) blocks all backdoor paths for $\{X, Y\}$, (2) blocks all backdoor paths for $\{M, Y\}$, (3) blocks all frontdoor paths for $\{X, Y\}$, and (4) does not open non-causal paths by conditioning on colliders. We use the language of *causal partitions* defined in Maasch et al. (2024).

1. **Backdoor paths for $\{X, Y\}$ are blocked.** Any confounder for $\{X, Y\}$ will be in causal partition \mathbf{Z}_1 , by definition of \mathbf{Z}_1 (Table 1; Maasch et al. 2024). All backdoor paths enter Y by definition (i.e., $\dots \rightarrow Y$). As \mathbf{A}_{DE} contains all confounders that are parents of Y , all backdoor paths for $\{X, Y\}$ will be blocked when conditioning on \mathbf{A}_{DE} .
2. **Backdoor paths for $\{M, Y\}$ are blocked.** Any confounder for M and Y will be in $\mathbf{Z}_1 \cup \mathbf{Z}_3 \cup \mathbf{Z}_4$ (e.g., Figure B.1), as these are the only causal partitions with edges pointing into Y . Set \mathbf{A}_{DE} by definition contains all members of $\mathbf{Z}_1, \mathbf{Z}_3$, and \mathbf{Z}_4 that are parents of Y .
3. **Frontdoor paths for $\{X, Y\}$ are blocked.** Any mediator for $\{X, Y\}$ will be in causal partition \mathbf{Z}_3 , by definition of \mathbf{Z}_3 (Table 1; Maasch et al. 2024). All frontdoor paths enter Y by definition (i.e., $\dots \rightarrow Y$). As \mathbf{A}_{DE} contains all mediators that are parents of Y , all frontdoor paths will be blocked.
4. **Non-causal paths through colliders are blocked.** Though \mathbf{Z} can contain colliders in $\mathbf{Z}_{2 \notin de(Y)}$, these cannot be parents of Y by definition. As defined, \mathbf{A}_{DE} does not contain any members of \mathbf{Z}_2 . Thus, non-causal paths will not be opened by conditioning on \mathbf{A}_{DE} .

□

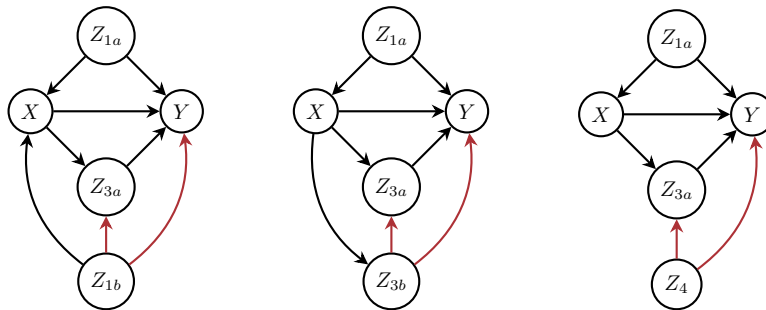


Figure B.1: Y and members of \mathbf{Z}_3 can be confounded by members of \mathbf{Z}_1 (e.g., left), \mathbf{Z}_3 (e.g., center), or \mathbf{Z}_4 (e.g., right), as these are the only causal partitions with edges pointing into Y .

C Empirical Validation on Synthetic and Semi-Synthetic Data

Computing Resources All experiments used an Apple MacBook (M2 Pro Chip; 12 CPU cores; 16G memory).

C.1 LD3 in the Presence of Latent Variables

We explored the impacts of latent variables that do and do not violate Assumption A2 (Table C.1). We iteratively dropped individual variables from the observed data represented by Figure C.1, including variables that do and do not act as confounders.

Results illustrate that (1) Theorem 1 holds and (2) Assumption A2 is sufficient but not necessary. WCDE for latent confounders B_1 , M_1 , and Z_{4a} remain unbiased, as these are not adjacent to Y (Theorem 1). Though latent M_2 could induce bias by allowing for the erroneous inclusion of M_3 in \mathbf{A}_{DE} , WCDE results are not significantly impacted in this setting. Additionally, though Z_{3c} is a parent of Y , dropping this variable simply causes LD3 to place its parent Z_{3b} in \mathbf{A}_{DE} . In this setting, the predicted \mathbf{A}_{DE} has 100% F1, precision, and recall with respect to the expected VAS, and the WCDE remains unbiased (1.25[1.24, 1.26]). Thus, Assumption A2 is sufficient but *not necessary* for returning a VAS.

LATENT	WCDE	SDC ACC	\mathbf{A}_{DE} F1	\mathbf{A}_{DE} PREC	\mathbf{A}_{DE} REC
$Z_1 \in \mathbf{Z}_1$	1.70 [1.66,1.75]	1.0	0.80 [0.80,0.80]	0.67 [0.67,0.67]	1.00 [1.00,1.00]
$B_1 \in \mathbf{Z}_1$	1.25 [1.24,1.26]	1.0	1.00 [1.00,1.00]	1.00 [1.00,1.00]	1.00 [1.00,1.00]
$B_2 \in \mathbf{Z}_1$	1.22 [1.17,1.27]	1.0	0.91 [0.89,0.93]	0.84 [0.81,0.86]	1.00 [1.00,1.00]
$B_3 \in \mathbf{Z}_1$	1.72 [1.68,1.76]	1.0	0.82 [0.8,0.840]	0.70 [0.67,0.73]	1.00 [1.00,1.00]
$M_1 \in \mathbf{Z}_5$	1.25 [1.24,1.26]	1.0	0.99 [0.98,1.01]	0.99 [0.96,1.01]	1.00 [1.00,1.00]
$M_2 \in \mathbf{Z}_4$	1.26 [1.25,1.26]	1.0	0.86 [0.86,0.86]	0.75 [0.75,0.75]	1.00 [1.00,1.00]
$Z_{4a} \in \mathbf{Z}_4$	1.25 [1.24,1.26]	1.0	1.00 [1.00,1.00]	1.00 [1.00,1.00]	1.00 [1.00,1.00]

Table C.1: Results with latent confounders. WCDE estimates (WCDE), SDC accuracy (ACC), \mathbf{A}_{DE} F1, \mathbf{A}_{DE} precision (PREC), and \mathbf{A}_{DE} recall (REC) for LD3 as confounders in Figure C.1 are iteratively dropped from the observed data (linear-Gaussian data; Fisher-z tests; $\alpha = 0.01$; true direct effect = 1.25). Values are means over 10 replicates with 95% confidence intervals in brackets. Latent nodes in red are adjacent to outcome Y , violating Assumption A2. \mathbf{A}_{DE} metrics were scored by comparing the set returned by LD3 to the true \mathbf{A}_{DE} set-minus the latent variable.

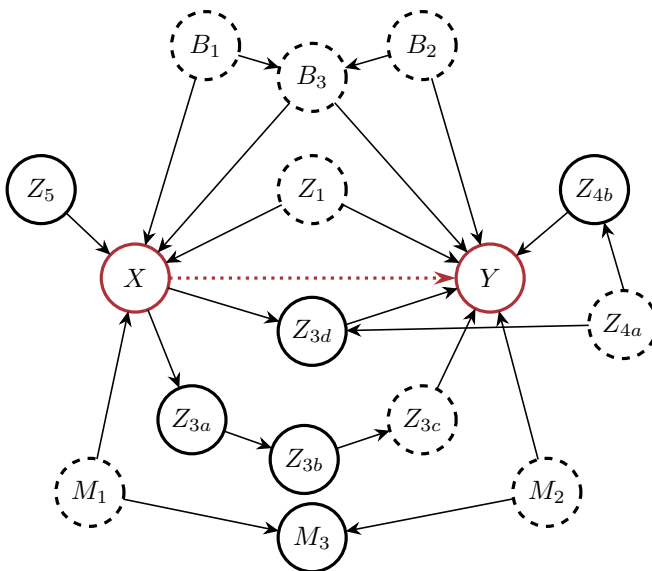


Figure C.1: Eighteen-node DAG used to evaluate the ability of LD3 to recover the true \mathbf{A}_{DE} , assess the SDC, and estimate the weighted CDE. For WCDE experiments (Figures C.3, C.4), all nodes were observed. For latent variable experiments (Section C.1), one dashed node was treated as latent per iteration.

C.2 Baseline Evaluation

Baseline Evaluation for Parent Discovery Baselines were evaluated on the basis of F1, precision, and recall with respect to the true parents of outcome Y (i.e., the members of \mathbf{A}_{DE}). Only LD3, LDECC, and MB-by-MB directly return the parents of Y . Additionally, PC, LDECC, and MB-by-MB return results relative to the MEC. Therefore, we evaluate each baseline with at least one form of post-processing to adjust for the task of \mathbf{A}_{DE} prediction. Post-processing is described below.

1. **NOTEARS**: Retain all parents of the Y in the unique graph.
2. **DirectLiNGAM**: Retain all parents of the Y in the unique graph.
3. **PC $_{\cap}$** : Retain the *intersection* of parent sets across DAGs in the MEC.
4. **PC $_{\cup}$** : Retain the *union* of parent sets across DAGs in the MEC.
5. **MB-by-MB**: Retain the variables labeled as parents of the target.
6. **LDECC $_{\cap}$** : Retain the variables labeled as parents of the target.
7. **LDECC $_{\cup}$** : Retain the variables labeled as parents of the target unioned with the variables adjacent to Y that are unoriented in the MEC.
8. **LDP**: Retain $\mathbf{Z}_1 \cup \mathbf{Z}_{POST} \cup \mathbf{Z}_4$. As our experimental setting requires that there are no descendants of the outcome, the superset $\mathbf{Z}_{POST} := \mathbf{Z}_{2 \in de(Y)} \cup \mathbf{Z}_3 \cup \mathbf{Z}_6$ defined in Maasch et al. (2024) will now only contain \mathbf{Z}_3 .
9. **LDP $_{pa}$** : Retain the variables that are not conditionally independent of Y given the remaining members of the set.

For the SANGIOVESE benchmark, we compared LD3 to NOTEARS, DirectLiNGAM, MB-by-MB, LDECC $_{\cap}$, PC $_{\cap}$, and LDP $_{pa}$. For ASIA and SACHS, we compared LD3 to PC $_{\cap}$, PC $_{\cup}$, LDECC $_{\cap}$, LDECC $_{\cup}$, LDP with no post-processing, and LDP $_{pa}$ to emphasize the impacts of different post-processing methods.

C.3 Erdős-Rényi Graphs

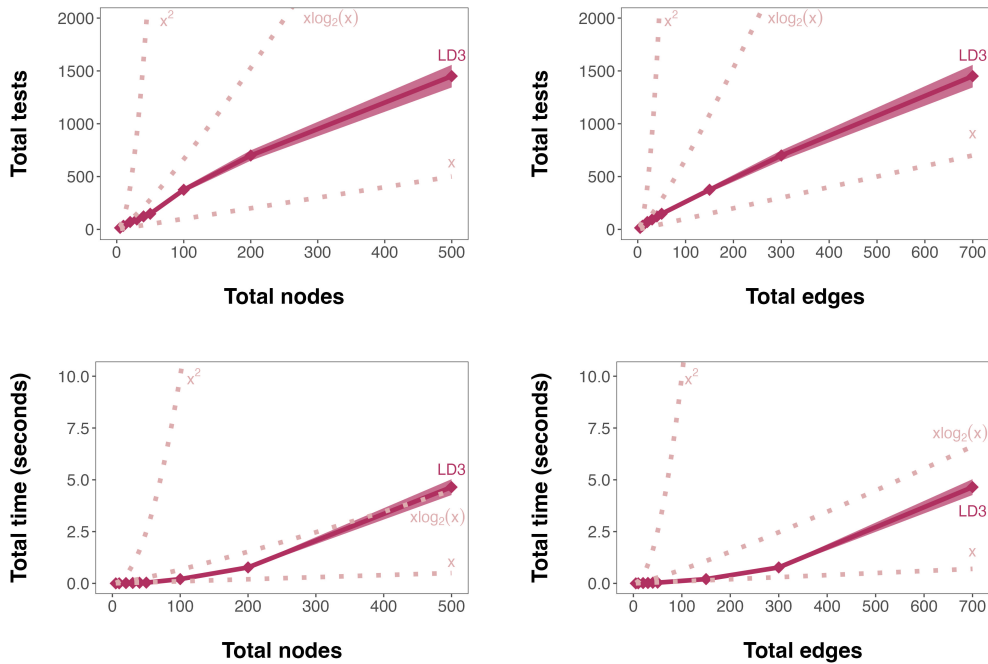


Figure C.2: Total runtime and total conditional independence tests performed with respect to total edges and total nodes, using an oracle on random directed acyclic Erdős-Rényi graphs (Erdős, Rényi et al. 1960).

C.4 Weighted CDE Estimation

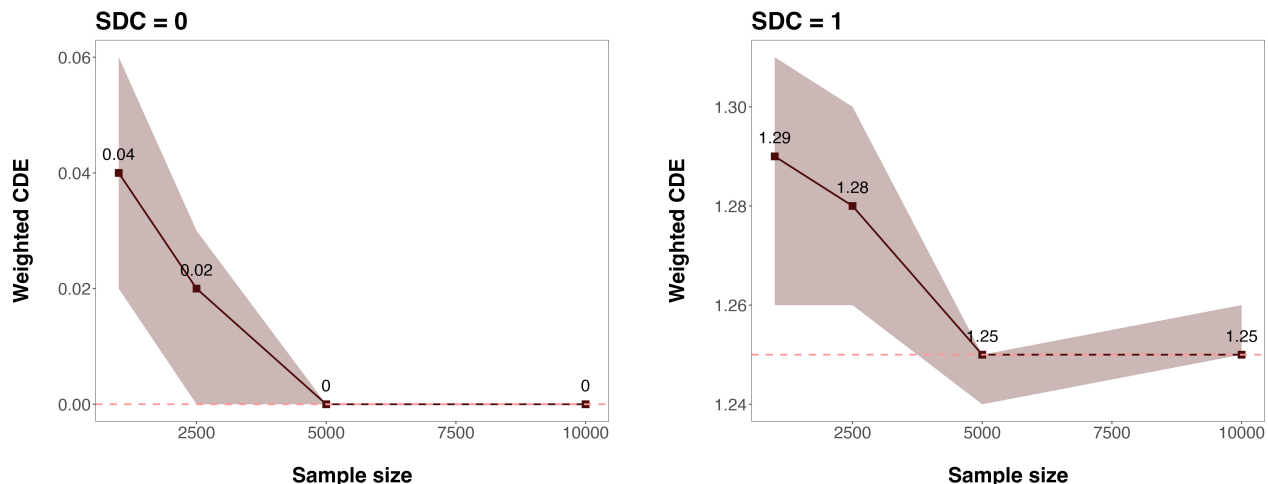


Figure C.3: Mean WCDE estimates over 100 replicates per sample size for linear-Gaussian instantiations of Figure C.1 (95% confidence intervals in shaded regions). Ground truth WCDE is denoted by the dashed line. LD3 used parametric Fisher-z tests ($\alpha = 0.01$), as the data generating process was known for this simulation. Estimates were obtained with linear regression (<https://scikit-learn.org/>). Note: This pipeline is for ease of explication in the illustrative setting only. For unknown data generating processes, we do not recommend this pipeline due to restrictive parametric assumptions.

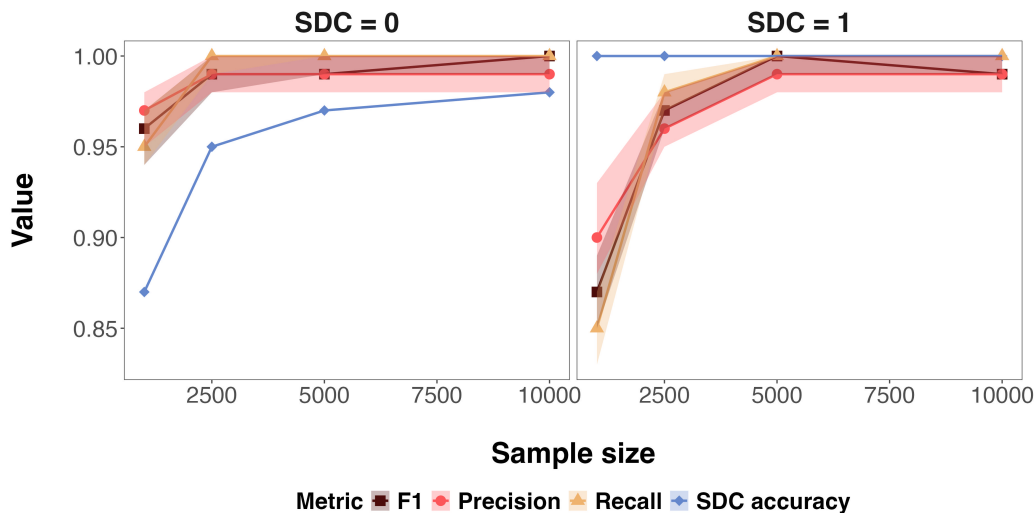


Figure C.4: SDC accuracy, A_{DE} F1, precision, and recall across sample sizes when SDC = 0 and SDC = 1. Values were averaged over 100 replicates of linear-Gaussian instantiations of Figure C.1, with 95% confidence intervals in shaded regions. LD3 used parametric Fisher-z tests ($\alpha = 0.01$), as the data generating process was known for this simulation.

C.5 Impacts of Unnecessary Adjustment

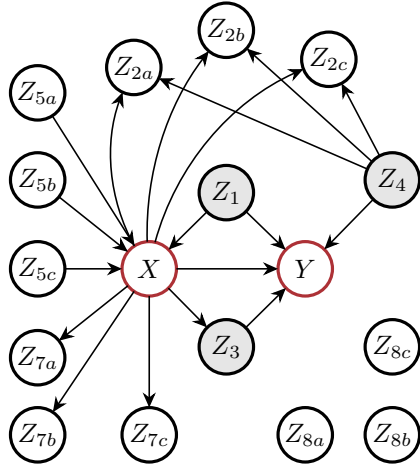


Figure C.5: The true \mathbf{A}_{DE} for X and Y is in gray.

n	ALL \mathbf{Z}		TRUE \mathbf{A}_{DE}		PRED \mathbf{A}_{DE}		
	Mean	Variance	Mean	Variance	Mean	Variance	\mathbf{A}_{DE} F1
500	0.239	0.052	0.347	0.004	0.344	0.004	0.99 [0.98,1.0]
1000	-0.011	0.038	0.35	0.003	0.349	0.003	0.99 [0.98,1.0]
10000	0.151	0.013	0.345	0.000	0.344	0.000	0.99 [0.98,1.0]

Table C.2: **Statistical Efficiency.** WCDE estimate mean and variance when adjusting for all \mathbf{Z} , the true \mathbf{A}_{DE} defined by our graphical criterion (TRUE \mathbf{A}_{DE}), and the predicted \mathbf{A}_{DE} returned by LD3 (PRED \mathbf{A}_{DE}) for the DAG in Figure C.5. Variance using all \mathbf{Z} was at least $12.6\times$ higher than using PRED \mathbf{A}_{DE} . F1 was high and variance for PRED \mathbf{A}_{DE} was equal to the variance using the ground truth \mathbf{A}_{DE} . Variables were categorical with quadratic causal functions. WCDE estimation used double machine learning using `econml` (<https://econml.azurewebsites.net/>) 100 replicates per sample size (95% confidence intervals in brackets). Though adjusting for all \mathbf{Z} will not theoretically induce bias in this setting, we see that mean WCDE values do diverge (and sometimes flip sign).

n	TRUE \mathbf{A}_{DE}		ALL \mathbf{Z}	
	Mean	Variance	Mean	Variance
100	6.98	0.83	6.97	7.79
1000	7.17	0.86	7.28	8.27
10000	6.91	1.16	7.25	9.04

Table C.3: **Statistical Efficiency.** Adjusting for all \mathbf{Z} in Figure C.5 results in high WCDE estimate variances, $7.8\times$ to $9.6\times$ higher than adjusting for \mathbf{A}_{DE} only. Data generating process was linear-Gaussian. TRUE \mathbf{A}_{DE} was selected according to the graphical criterion introduced in this work. WCDE estimation used linear regression with 100 replicates per sample size (<https://scikit-learn.org/>). True WCDE was 7.

	n	$ \mathbf{Z} $	$ \mathbf{A}_{DE} $	Acc	F1	Rec	Prec	Time
ECOLI	1k	44	2.0 [2.0,2.0]	1.00 [1.00,1.00]	1.00 [1.00,1.00]	1.00 [1.00,1.00]	1.00 [1.00,1.00]	0.016 [0.01,0.021]
ANDES	50k	221	4.5 [4.06,4.94]	1.00 [1.00,1.00]	0.95 [0.9,0.99]	0.91 [0.83,0.99]	1.00 [1.00,1.00]	0.76 [0.737,0.784]

Table C.4: **Interpretability.** \mathbf{A}_{DE} discovered by LD3 can provide greater interpretability than adjusting for all \mathbf{Z} , especially in large DAGs. We used the binary ANDES (Conati et al. 1997) and Gaussian ECOLI (Schäfer and Strimmer 2005) benchmarks from `bnlearn` (Scutari 2010). When the true parent set is small but total number of nodes is moderate (e.g., ECOLI) to large (e.g., ANDES), forgoing structure learning by adjusting for \mathbf{Z} is a missed opportunity to provide mechanistic insights (e.g., causal fairness mechanisms). In the fairness setting, we can draw direct discrimination conclusions about the members of \mathbf{A}_{DE} , but not \mathbf{Z} alone. On average, eliminating extraneous variables took less than one second. ECOLI used Fisher-z tests ($\alpha = 0.001$) and ANDES used χ^2 ($\alpha = 0.01$). Values were averaged over ten replicates (95% confidence intervals in brackets).

C.6 bnlearn Benchmarks

n	METHOD	TIME	INDEPENDENCE TESTS	ACCURACY	F1	PRECISION	RECALL
250	LD3	0.005 [0.003,0.008]	60.8 [60.41,61.19]	0.74 [0.71,0.78]	0.7 [0.65,0.76]	1.00 [1.00,1.00]	0.55 [0.48,0.62]
	LDECC	0.092 [0.063,0.12]	316.6 [220.98,412.22]	0.61 [0.55,0.67]	0.47 [0.33,0.6]	0.9 [0.7,1.0]	0.32 [0.2,0.43]
	MB-by-MB	0.092 [0.047,0.136]	268.4 [179.54,357.26]	0.63 [0.57,0.68]	0.5 [0.37,0.62]	0.9 [0.7,1.0]	0.35 [0.25,0.45]
	LDP	0.009 [0.006,0.012]	112.1 [90.82,133.38]	0.76 [0.72,0.81]	0.76 [0.71,0.8]	0.94 [0.87,1.0]	0.64 [0.59,0.68]
	PC	0.118 [0.099,0.136]	557.9 [524.73,591.07]	0.64 [0.58,0.69]	0.51 [0.39,0.64]	0.9 [0.7,1.0]	0.36 [0.27,0.46]
	DirectLiNGAM	0.142 [0.138,0.145]	-	0.63 [0.55,0.7]	0.56 [0.43,0.69]	0.85 [0.75,0.95]	0.48 [0.32,0.63]
	NOTEARS	1.216 [0.985,1.447]	-	0.79 [0.75,0.82]	0.79 [0.75,0.82]	0.91 [0.86,0.96]	0.7 [0.65,0.75]
500	LD3	0.006 [0.004,0.008]	60.8 [60.41,61.19]	0.85 [0.79,0.91]	0.84 [0.77,0.91]	1.00 [1.00,1.00]	0.74 [0.64,0.84]
	LDECC	0.137 [0.104,0.169]	458.2 [354.85,561.55]	0.68 [0.63,0.73]	0.6 [0.52,0.69]	0.98 [0.94,1.0]	0.45 [0.37,0.53]
	MB-by-MB	0.127 [0.113,0.141]	370 [328.41,411.59]	0.64 [0.61,0.68]	0.55 [0.48,0.61]	0.98 [0.94,1.0]	0.39 [0.32,0.46]
	LDP	0.01 [0.005,0.016]	84.3 [66.81,101.79]	0.78 [0.73,0.82]	0.77 [0.72,0.82]	0.94 [0.88,1.0]	0.66 [0.6,0.73]
	PC	0.181 [0.162,0.201]	879.6 [843.24,915.96]	0.61 [0.56,0.67]	0.47 [0.38,0.57]	1.00 [1.00,1.00]	0.32 [0.23,0.42]
	DirectLiNGAM	0.152 [0.144,0.16]	-	0.56 [0.46,0.67]	0.42 [0.18,0.65]	0.43 [0.19,0.67]	0.41 [0.18,0.65]
	NOTEARS	1.092 [1.025,1.158]	-	0.79 [0.76,0.82]	0.78 [0.75,0.81]	0.95 [0.9,1.0]	0.66 [0.63,0.7]
1000	LD3	0.009 [0.007,0.011]	61 [61,61]	0.97 [0.95,0.99]	0.99 [0.95,0.99]	1.00 [1.00,1.00]	0.95 [0.91,0.99]
	LDECC	0.217 [0.185,0.248]	669.3 [560.92,777.68]	0.66 [0.61,0.72]	0.57 [0.45,0.68]	1.00 [1.00,1.00]	0.41 [0.31,0.52]
	MB-by-MB	0.201 [0.175,0.228]	592.7 [538.57,646.83]	0.69 [0.66,0.72]	0.63 [0.58,0.68]	1.00 [1.00,1.00]	0.46 [0.41,0.51]
	LDP	0.006 [0.003,0.009]	75 [63.46,86.54]	0.95 [0.91,0.99]	0.95 [0.91,0.99]	0.99 [0.96,1.0]	0.92 [0.87,0.98]
	PC	0.289 [0.272,0.306]	1333.9 [1249.08,1418.72]	0.55 [0.5,0.6]	0.33 [0.21,0.45]	0.8 [0.54,1.06]	0.21 [0.13,0.29]
	DirectLiNGAM	0.366 [0.326,0.407]	-	0.62 [0.55,0.69]	0.56 [0.4,0.73]	0.66 [0.51,0.8]	0.54 [0.34,0.73]
	NOTEARS	1.694 [1.571,1.818]	-	0.8 [0.77,0.83]	0.79 [0.75,0.82]	1.00 [1.00,1.00]	0.65 [0.6,0.7]

Table C.5: Results on the SANGIOVESE benchmark from bnlearn (Scutari 2010), a linear-Gaussian model of Tuscan Sangiovese grape production (Magrini, Di Blasi, and Stefanini 2017). Ten replicate datasets were sampled at $n = [250, 500, 1000]$. Means are given with 95% confidence intervals in brackets. Exposure was PH and outcome was GRAPEW. All constraint-based methods used Fisher-z tests ($\alpha = 0.01$). NOTEARS hyper-parameters were $\lambda_1 = 0.001$ and loss type l_2 . DirectLiNGAM: <https://lingam.readthedocs.io/>; PC, LDECC, MB-by-MB: <https://github.com/acmi-lab/local-causal-discovery>; NOTEARS: <https://github.com/xunzheng/notears>; LDP: <https://github.com/jmaasch/ldp>.

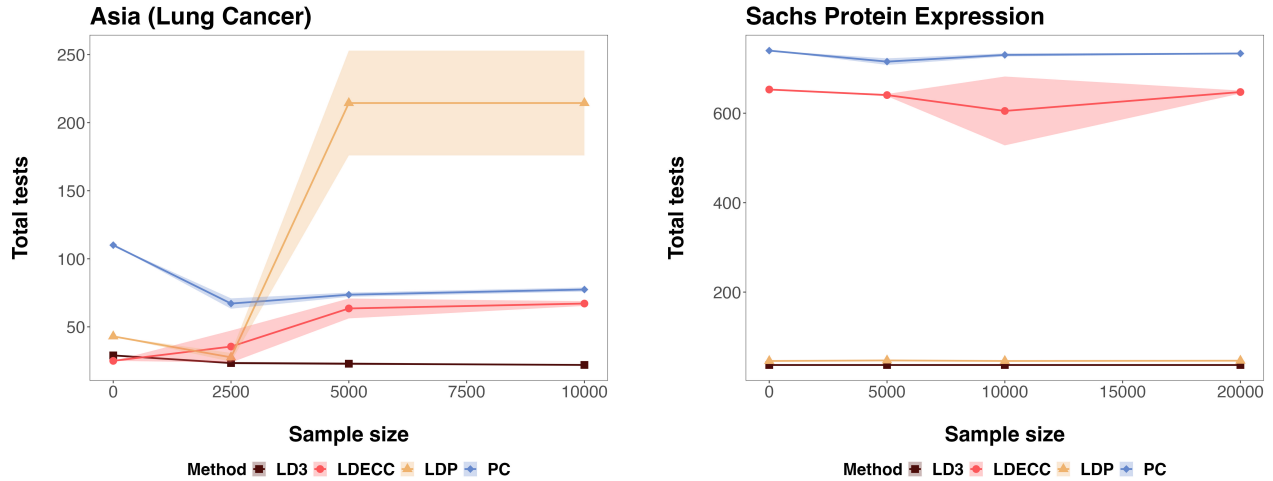


Figure C.6: Total number of independence tests performed for the ASIA (Lauritzen and Spiegelhalter 1988) and SACHS (Sachs et al. 2005) benchmarks from bnlearn (<https://www.bnlearn.com/bnrepository/>) (Scutari 2010) (χ^2 tests; $\alpha = 0.001$; 95% confidence intervals in shaded regions). For ASIA (EITHER \rightarrow DYSP), $|\mathbf{Z}| = 6$ and $|\mathbf{A}_{DE}| = 1$. For SACHS (ERK \rightarrow AKT), $|\mathbf{Z}| = 11$ and $|\mathbf{A}_{DE}| = 1$. Raw data are reported in Tables C.7 and C.9.

		ASIA (LUNG CANCER)						
		SDC = 1: either \rightarrow dysp			SDC = 0: xray $\not\rightarrow$ dysp			
		<i>F1</i>	<i>Prec</i>	<i>Rec</i>	<i>F1</i>	<i>Prec</i>	<i>Rec</i>	
<i>Oracle</i>	LD3	1.00	1.00	1.00	1.00	1.00	1.00	1.00
	PC _U	1.00	1.00	1.00	1.00	1.00	1.00	1.00
	PC _n	1.00	1.00	1.00	1.00	1.00	1.00	1.00
	LDECC _U	1.00	1.00	1.00	1.00	1.00	1.00	1.00
	LDECC _n	1.00	1.00	1.00	1.00	1.00	1.00	1.00
	LDP _{pa}	1.00	1.00	1.00	1.00	1.00	1.00	1.00
	LDP	0.50	0.33	1.00	0.67	0.50	1.00	1.00
$n = 2.5k$	LD3	1.00 [1.00,1.00]	1.00 [1.00,1.00]	1.00 [1.00,1.00]	0.80 [0.69,0.91]	1.00 [1.00,1.00]	0.70 [0.54,0.86]	
	PC _U	0.00 [0.00,0.00]	0.00 [0.00,0.00]	0.00 [0.00,0.00]	0.00 [0.00,0.00]	0.00 [0.00,0.00]	0.00 [0.00,0.00]	0.00 [0.00,0.00]
	PC _n	0.00 [0.00,0.00]	0.00 [0.00,0.00]	0.00 [0.00,0.00]	0.00 [0.00,0.00]	0.00 [0.00,0.00]	0.00 [0.00,0.00]	0.00 [0.00,0.00]
	LDECC _U	0.75 [0.61,0.89]	0.65 [0.46,0.84]	1.00 [1.00,1.00]	0.67 [0.49,0.85]	0.65 [0.46,0.84]	0.70 [0.54,0.86]	
	LDECC _n	0.75 [0.61,0.89]	0.65 [0.46,0.84]	1.00 [1.00,1.00]	0.67 [0.49,0.85]	0.65 [0.46,0.84]	0.70 [0.54,0.86]	
	LDP _{pa}	1.00 [1.00,1.00]	1.00 [1.00,1.00]	1.00 [1.00,1.00]	0.83 [0.72,0.94]	1.00 [1.00,1.00]	0.75 [0.59,0.91]	
	LDP	0.26 [0.24,0.28]	0.15 [0.14,0.16]	0.97 [0.90,1.00]	0.14 [0.13,0.14]	0.07 [0.07,0.08]	1.00 [1.00,1.00]	
$n = 5k$	LD3	1.00 [1.00,1.00]	1.00 [1.00,1.00]	1.00 [1.00,1.00]	0.90 [0.80,1.00]	1.00 [1.00,1.00]	0.85 [0.70,1.00]	
	PC _U	0.00 [0.00,0.00]	0.00 [0.00,0.00]	0.00 [0.00,0.00]	0.00 [0.00,0.00]	0.00 [0.00,0.00]	0.00 [0.00,0.00]	0.00 [0.00,0.00]
	PC _n	0.00 [0.00,0.00]	0.00 [0.00,0.00]	0.00 [0.00,0.00]	0.00 [0.00,0.00]	0.00 [0.00,0.00]	0.00 [0.00,0.00]	0.00 [0.00,0.00]
	LDECC _U	0.60 [0.47,0.73]	0.47 [0.29,0.64]	1.00 [1.00,1.00]	0.52 [0.36,0.68]	0.47 [0.29,0.64]	0.60 [0.47,0.73]	
	LDECC _n	0.60 [0.47,0.73]	0.47 [0.29,0.64]	1.00 [1.00,1.00]	0.52 [0.36,0.68]	0.47 [0.29,0.64]	0.60 [0.47,0.73]	
	LDP _{pa}	1.00 [1.00,1.00]	1.00 [1.00,1.00]	1.00 [1.00,1.00]	0.93 [0.85,1.00]	1.00 [1.00,1.00]	0.90 [0.77,1.00]	
	LDP	0.65 [0.62,0.68]	0.48 [0.45,0.52]	1.00 [1.00,1.00]	0.65 [0.62,0.67]	0.48 [0.45,0.51]	1.00 [1.00,1.00]	
$n = 10k$	LD3	1.00 [1.00,1.00]	1.00 [1.00,1.00]	1.00 [1.00,1.00]	0.90 [0.80,1.00]	1.00 [1.00,1.00]	0.85 [0.70,1.00]	
	PC _U	0.00 [0.00,0.00]	0.00 [0.00,0.00]	0.00 [0.00,0.00]	0.00 [0.00,0.00]	0.00 [0.00,0.00]	0.00 [0.00,0.00]	0.00 [0.00,0.00]
	PC _n	0.00 [0.00,0.00]	0.00 [0.00,0.00]	0.00 [0.00,0.00]	0.00 [0.00,0.00]	0.00 [0.00,0.00]	0.00 [0.00,0.00]	0.00 [0.00,0.00]
	LDECC _U	0.50 [0.50,0.50]	0.33 [0.33,0.33]	0.00 [0.00,0.00]	0.40 [0.40,0.40]	0.33 [0.33,0.33]	0.50 [0.50,0.50]	
	LDECC _n	0.50 [0.50,0.50]	0.33 [0.33,0.33]	0.00 [0.00,0.00]	0.40 [0.40,0.40]	0.33 [0.33,0.33]	0.50 [0.50,0.50]	
	LDP _{pa}	1.00 [1.00,1.00]	1.00 [1.00,1.00]	1.00 [1.00,1.00]	0.90 [0.80,1.00]	1.00 [1.00,1.00]	0.85 [0.70,1.00]	
	LDP	0.67 [0.67,0.67]	0.50 [0.50,0.50]	1.00 [1.00,1.00]	0.64 [0.61,0.67]	0.47 [0.44,0.5]	1.00 [1.00,1.00]	

Table C.6: Empirical performance on the ASIA (Lung Cancer) Bayesian network dataset (Lauritzen 1988) from bnlearn (Scutari 2010). Binary data were evaluated with χ^2 independence tests ($\alpha = 0.001$; 95% confidence intervals in brackets). Unexpected decreases in baseline performance for increasing sample size might be due to the difficulty of this dataset for structure learning, as noted in the bnlearn documentation: “Standard learning algorithms are not able to recover the true structure of the network because of the presence of a node (E) with conditional probabilities equal to both 0 and 1” (<https://www.bnlearn.com/documentation/man/asia.html>).

		ASIA (LUNG CANCER)			
		SDC = 1: either \rightarrow dysp		SDC = 0: xray \nrightarrow dysp	
		<i>Time</i>	<i>Tests</i>	<i>Time</i>	<i>Tests</i>
<i>Oracle</i>	LD3	0.002	29	0.002	31
	PC	0.007	110	0.007	115
	LDECC	0.003	25	0.004	25
	LDP	0.003	43	0.003	50
$n = 2.5k$	LD3	0.003 [0.002,0.003]	23.4 [22.56,24.24]	0.003 [0.003,0.003]	27.2 [26.56,27.84]
	PC	0.032 [0.03,0.034]	67.1 [63.31,70.89]	0.033 [0.031,0.035]	70.5 [66.79,74.21]
	LDECC	0.024 [0.016,0.033]	35.5 [23.78,47.22]	0.018 [0.013,0.023]	35.5 [23.78,47.22]
	LDP	0.003 [0.003,0.003]	27.6 [24.41,30.79]	0.003 [0.003,0.003]	31.0 [27.94,34.06]
$n = 5k$	LD3	0.004 [0.003,0.004]	22.9 [21.96,23.84]	0.004 [0.003,0.004]	26.6 [26.0,27.2]
	PC	0.056 [0.054,0.057]	73.6 [72.02,75.18]	0.058 [0.057,0.06]	77.1 [75.29,78.91]
	LDECC	0.049 [0.044,0.054]	63.5 [56.21,70.79]	0.047 [0.042,0.053]	63.5 [56.21,70.79]
	LDP	0.073 [0.056,0.091]	214.4 [175.9,252.9]	0.039 [0.033,0.044]	192.0 [167.74,216.26]
$n = 10k$	LD3	0.004 [0.004,0.004]	22.0 [22.0,22.0]	0.005 [0.005,0.005]	26.6 [26.0,27.2]
	PC	0.100 [0.097,0.103]	77.4 [75.9,78.9]	0.105 [0.102,0.109]	82.3 [80.38,84.22]
	LDECC	0.096 [0.083,0.109]	67.1 [65.34,68.86]	0.087 [0.084,0.09]	67.1 [65.34,68.86]
	LDP	0.073 [0.056,0.091]	214.4 [175.9,252.9]	0.039 [0.033,0.044]	192.0 [167.74,216.26]

Table C.7: Total number of independence tests performed and runtimes in seconds (95% confidence intervals in brackets).

		SACHS PROTEIN EXPRESSION					
		SDC = 1: ERK \rightarrow AKT			SDC = 0: JNK \nrightarrow P38		
		<i>Fl</i>	<i>Prec</i>	<i>Rec</i>	<i>Fl</i>	<i>Prec</i>	<i>Rec</i>
<i>Oracle</i>	LD3	1.00	1.00	1.00	1.00	1.00	1.00
	PC _U	1.00	1.00	1.00	1.00	1.00	1.00
	PC _N	0.00	0.00	0.00	0.00	0.00	0.00
	LDECC _U	1.00	1.00	1.00	1.00	1.00	1.00
	LDECC _N	0.00	0.00	0.00	0.00	0.00	0.00
	LDP _{pa}	1.00	1.00	1.00	1.00	1.00	1.00
	LDP	0.29	0.16	1.00	0.50	0.33	1.00
$n = 5k$	LD3	0.97 [0.90,1.00]	0.95 [0.85,1.00]	1.00 [1.00,1.00]	0.96 [0.91,1.00]	0.93 [0.85,1.00]	1.00 [1.00,1.00]
	PC _U	0.00 [0.00,0.00]	0.00 [0.00,0.00]	0.00 [0.00,0.00]	0.77 [0.51,1.00]	0.80 [0.54,1.00]	0.75 [0.49,1.00]
	PC _N	0.00 [0.00,0.00]	0.00 [0.00,0.00]	0.00 [0.00,0.00]	0.73 [0.48,0.99]	0.80 [0.54,1.00]	0.70 [0.44,0.96]
	LDECC _U	1.00 [1.00,1.00]	1.00 [1.00,1.00]	1.00 [1.00,1.00]	1.00 [1.00,1.00]	1.00 [1.00,1.00]	1.00 [1.00,1.00]
	LDECC _N	0.10 [-0.1,0.30]	0.10 [-0.1,0.30]	0.10 [-0.1,0.30]	0.10 [-0.1,0.30]	0.10 [-0.1,0.30]	0.10 [-0.1,0.30]
	LDP _{pa}	0.93 [0.85,1.02]	0.90 [0.77,1.00]	1.00 [1.00,1.00]	0.96 [0.91,1.00]	0.93 [0.85,1.00]	1.00 [1.00,1.00]
	LDP	0.29 [0.29,0.29]	0.17 [0.17,0.17]	1.00 [1.00,1.00]	0.50 [0.50,0.50]	0.33 [0.33,0.33]	1.00 [1.00,1.00]
$n = 10k$	LD3	1.00 [1.00,1.00]	1.00 [1.00,1.00]	1.00 [1.00,1.00]	1.00 [1.00,1.00]	1.00 [1.00,1.00]	1.00 [1.00,1.00]
	PC _U	0.50 [0.17,0.83]	0.50 [0.17,0.83]	0.50 [0.17,0.83]	1.00 [1.00,1.00]	1.00 [1.00,1.00]	1.00 [1.00,1.00]
	PC _N	0.00 [0.00,0.00]	0.00 [0.00,0.00]	0.00 [0.00,0.00]	0.47 [0.16,0.78]	0.50 [0.17,0.83]	0.45 [0.14,0.76]
	LDECC _U	1.00 [1.00,1.00]	1.00 [1.00,1.00]	1.00 [1.00,1.00]	1.00 [1.00,1.00]	1.00 [1.00,1.00]	1.00 [1.00,1.00]
	LDECC _N	0.10 [-0.1,0.30]	0.10 [-0.1,0.30]	0.10 [-0.1,0.30]	0.30 [0.00,0.60]	0.30 [0.00,0.60]	0.30 [0.00,0.60]
	LDP _{pa}	1.00 [1.00,1.00]	1.00 [1.00,1.00]	1.00 [1.00,1.00]	1.00 [1.00,1.00]	1.00 [1.00,1.00]	1.00 [1.00,1.00]
	LDP	0.29 [0.29,0.29]	0.17 [0.17,0.17]	1.00 [1.00,1.00]	0.50 [0.50,0.50]	0.33 [0.33,0.33]	1.00 [1.00,1.00]
$n = 20k$	LD3	0.97 [0.90,1.00]	0.95 [0.85,1.00]	1.00 [1.00,1.00]	1.00 [1.00,1.00]	1.00 [1.00,1.00]	1.00 [1.00,1.00]
	PC _U	0.90 [0.70,1.00]	0.90 [0.70,1.00]	0.90 [0.70,1.00]	1.00 [1.00,1.00]	1.00 [1.00,1.00]	1.00 [1.00,1.00]
	PC _N	0.00 [0.00,0.00]	0.00 [0.00,0.00]	0.00 [0.00,0.00]	0.10 [-0.1,0.30]	0.10 [-0.1,0.30]	0.10 [-0.1,0.30]
	LDECC _U	1.00 [1.00,1.00]	1.00 [1.00,1.00]	1.00 [1.00,1.00]	1.00 [1.00,1.00]	1.00 [1.00,1.00]	1.00 [1.00,1.00]
	LDECC _N	0.00 [0.00,0.00]	0.00 [0.00,0.00]	0.00 [0.00,0.00]	0.00 [0.00,0.00]	0.00 [0.00,0.00]	0.00 [0.00,0.00]
	LDP _{pa}	0.97 [0.90,1.00]	0.95 [0.85,1.00]	1.00 [1.00,1.00]	1.00 [1.00,1.00]	1.00 [1.00,1.00]	1.00 [1.00,1.00]
	LDP	0.29 [0.29,0.29]	0.17 [0.17,0.17]	1.00 [1.00,1.00]	0.50 [0.50,0.50]	0.33 [0.33,0.33]	1.00 [1.00,1.00]

Table C.8: Performance on the SACHS protein dataset (Sachs et al. 2005) from bnlearn (Scutari 2010). Discrete data were evaluated with χ^2 independence tests ($\alpha = 0.001$; 95% confidence intervals in brackets).

SACHS PROTEIN EXPRESSION					
		SDC = 1: ERK → AKT		SDC = 0: JNK ↯ P38	
		<i>Time</i>	<i>Tests</i>	<i>Time</i>	<i>Tests</i>
<i>Oracle</i>	LD3	0.013	37	0.013	37
	PC	0.077	740	0.079	740
	LDECC	0.079	653	0.081	646
	LDP	0.017	46	0.017	52
$n = 5k$	LD3	0.005 [0.005,0.006]	37.0 [37.0,37.0]	0.005 [0.005,0.005]	37.0 [37.0,37.0]
	PC	0.738 [0.729,0.747]	715.4 [708.08,722.72]	0.757 [0.741,0.773]	715.4 [708.08,722.72]
	LDECC	0.699 [0.688,0.709]	640.6 [638.15,643.05]	0.657 [0.596,0.718]	604.7 [550.92,658.48]
	LDP	0.006 [0.006,0.006]	47.2 [45.63,48.77]	0.009 [0.004,0.015]	52.4 [51.88,52.92]
$n = 10k$	LD3	0.007 [0.007,0.007]	37.0 [37.0,37.0]	0.007 [0.006,0.007]	37.0 [37.0,37.0]
	PC	1.388 [1.374,1.402]	730.4 [726.86,733.94]	1.394 [1.384,1.405]	730.4 [726.86,733.94]
	LDECC	1.199 [1.045,1.353]	605.1 [528.14,682.06]	1.041 [0.83,1.253]	536.7 [428.01,645.39]
	LDP	0.008 [0.008,0.008]	46.0 [46.0,46.0]	0.008 [0.008,0.009]	52.0 [52.0,52.0]
$n = 20k$	LD3	0.011 [0.011,0.011]	37.0 [37.0,37.0]	0.011 [0.01,0.011]	37.0 [37.0,37.0]
	PC	2.718 [2.689,2.746]	733.6 [732.19,735.01]	2.72 [2.676,2.763]	733.6 [732.19,735.01]
	LDECC	2.5 [2.451,2.549]	647.4 [644.05,650.75]	2.472 [2.438,2.506]	644.4 [641.0,647.8]
	LDP	0.012 [0.012,0.013]	46.6 [45.42,47.78]	0.013 [0.013,0.013]	52.0 [52.0,52.0]

Table C.9: Total number of independence tests and runtimes (95% confidence intervals in brackets).

D Causal Fairness Experiments

Computing Resources All causal fairness experiments used an Apple MacBook (M2 Pro Chip; 12 CPU cores; 16G memory).

D.1 COMPAS Recidivism Prediction

Data Preprocessing We used the data file `compas-scores-two-years.csv` from ProPublica,⁸ retaining the following columns for our analyses:

1. `race` (float64)
2. `sex` (float64)
3. `age_cat` (float64)
4. `juv_fel_count` (int64)
5. `juv_misd_count` (int64)
6. `juv_other_count` (int64)
7. `priors_count` (int64)
8. `c_charge_degree` (float64)
9. `two_year_recid` (int64)
10. `decile_score` (int64)
11. `race_binary` (int64)

Race was filtered to retain African American ($n = 3696$) and white individuals ($n = 2454$). For each exposure-outcome pair, $|\mathbf{Z}| = 7$. When exposure was `race` and outcome was `decile_score`, \mathbf{Z} contained all features other than `two_year_recid` (as this temporally proceeds `decile_score`, violating A1). When exposure was `race` and outcome was `two_year_recid`, \mathbf{Z} contained all features other than `decile_score`.

	WHITE ($n = 2454$)	AFRICAN AMERICAN ($n = 3696$)
<i>Age</i>	37.73 (12.76)	32.74 (10.86)
<i>Charge degree (felony)</i>	0.6 (0.49)	0.69 (0.46)
<i>Charge degree (misdemeanor)</i>	0.4 (0.49)	0.31 (0.46)
<i>General recidivism decile score</i>	3.74 (2.6)	5.37 (2.83)
<i>Juvenile felony count</i>	0.03 (0.3)	0.1 (0.51)
<i>Juvenile misdemeanor count</i>	0.04 (0.28)	0.14 (0.61)
<i>Juvenile other count</i>	0.09 (0.45)	0.14 (0.56)
<i>Priors count</i>	2.59 (3.8)	4.44 (5.58)
<i>Sex (female)</i>	0.23 (0.42)	0.18 (0.38)
<i>Sex (male)</i>	0.77 (0.42)	0.82 (0.38)
<i>Two-year recidivism (no)</i>	0.61 (0.49)	0.49 (0.5)
<i>Two-year recidivism (yes)</i>	0.39 (0.49)	0.51 (0.5)

Table D.1: Summary statistics for African American versus white individuals in the COMPAS dataset after preprocessing. We report mean values (standard deviations).

⁸<https://github.com/propublica/compas-analysis>

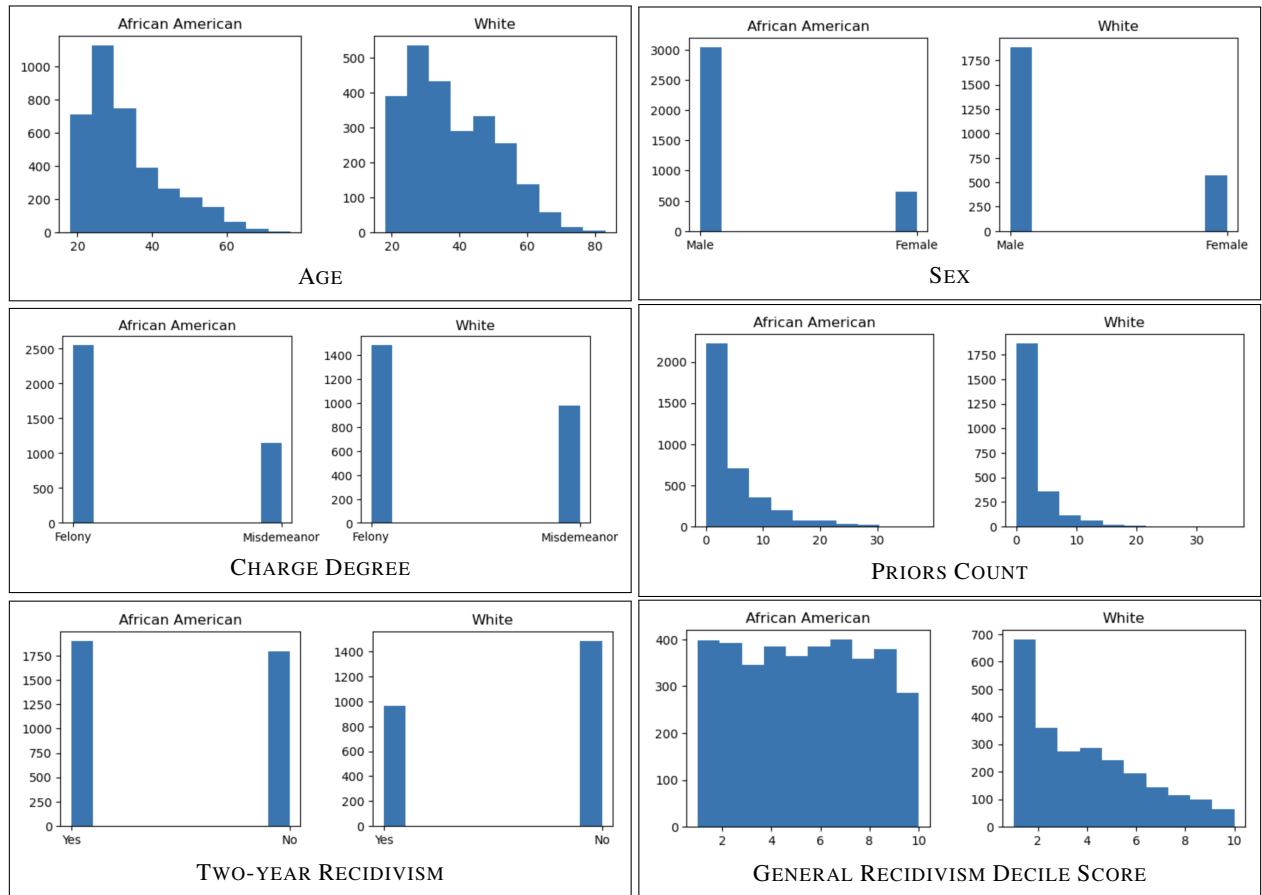


Figure D.1: Distributions for African American versus white individuals in the COMPAS dataset after preprocessing.

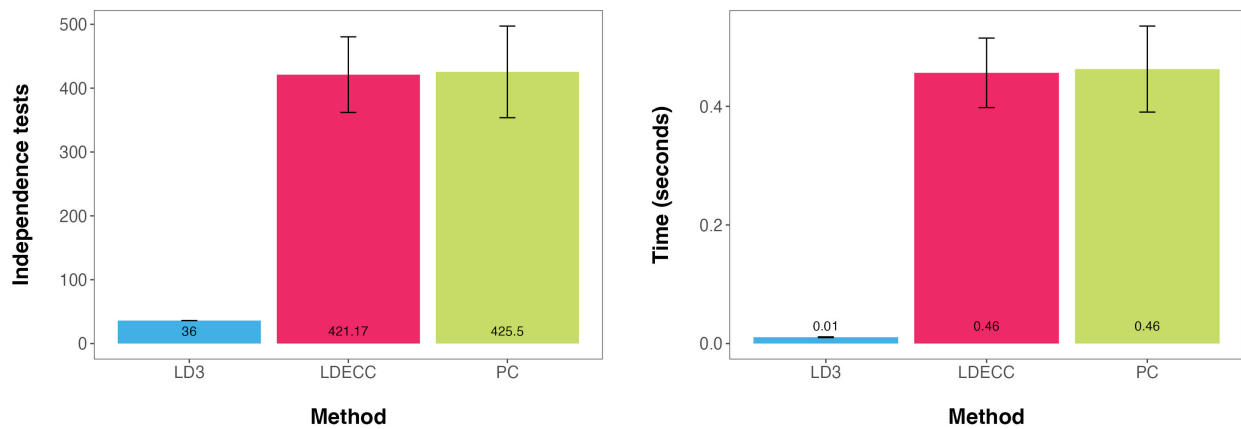


Figure D.2: Average number of independence tests performed and average time (seconds) per method on COMPAS experiments.

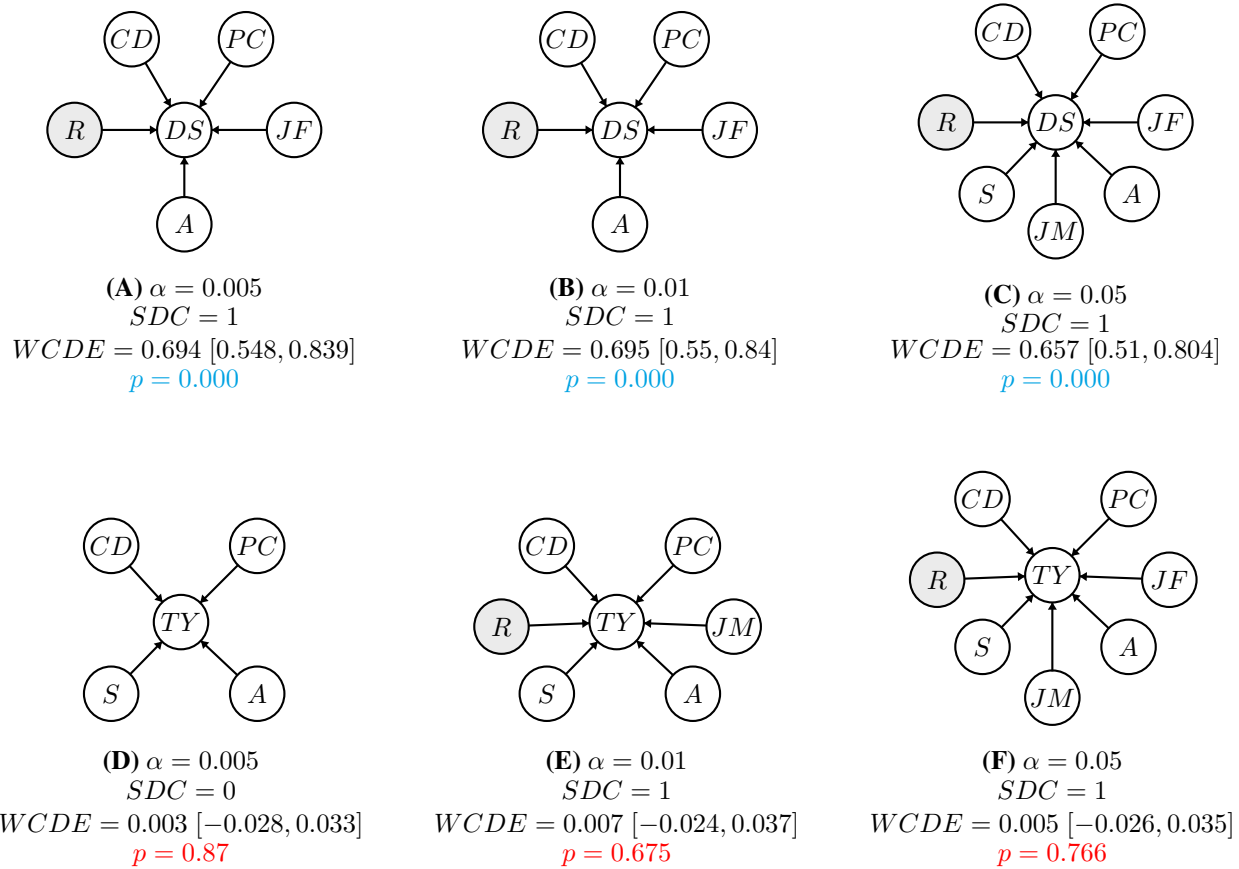


Figure D.3: LD3 results on the COMPAS dataset at different significance levels ($\alpha = [0.005, 0.01, 0.05]$). DAGs represent the predicted parent set for the outcome only, with all other relations abstracted away. (A–C) Exposure race and outcome general recidivism decile score. (D–F) Exposure race and outcome two-year recidivism. A = age; CD = charge degree; DS = decile score; JF = juvenile felony count; JM = juvenile misdemeanor count; PC = priors count; R = race; S = sex; TY = two-year recidivism. Weighted CDE (WCDE) is reported with p -value (p) and 95% confidence intervals in brackets.

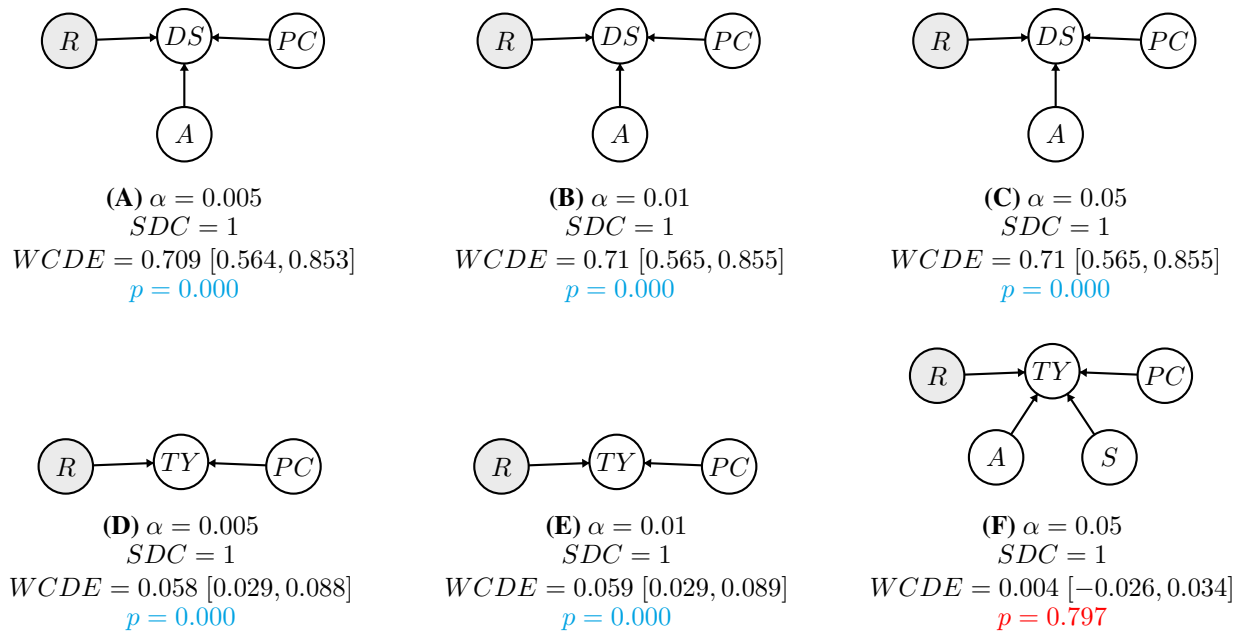


Figure D.4: PC results on the COMPAS dataset at different significance levels ($\alpha = [0.005, 0.01, 0.05]$). DAGs represent the predicted parent set for the outcome only, with all other relations abstracted away. (A–C) Exposure race and outcome general recidivism decile score. (D–F) Exposure race and outcome two-year recidivism. A = age; DS = decile score; PC = priors count; R = race; S = sex; TY = two-year recidivism. Weighted CDE ($WCDE$) is reported with p -value (p) and 95% confidence intervals in brackets.

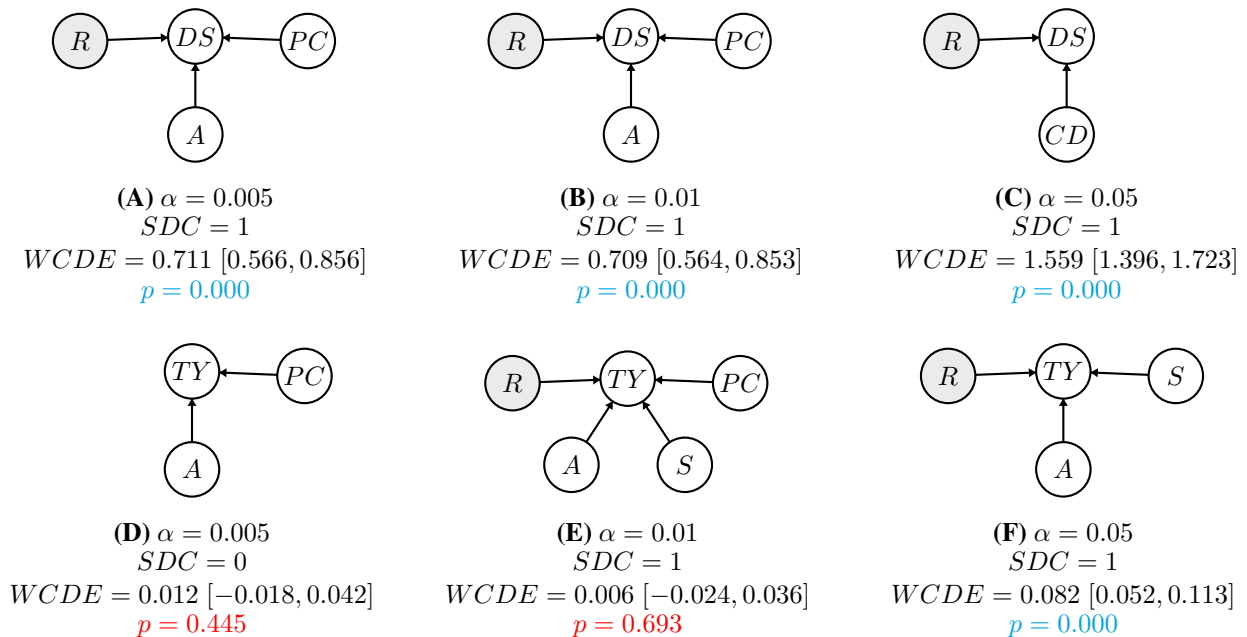


Figure D.5: LDECC results on the COMPAS dataset at different significance levels ($\alpha = [0.005, 0.01, 0.05]$). DAGs represent the predicted parent set for the outcome only, with all other relations abstracted away. (A–C) Exposure race and outcome general recidivism decile score. (D–F) Exposure race and outcome two-year recidivism. A = age; CD = charge degree; DS = decile score; PC = priors count; R = race; S = sex; TY = two-year recidivism. Weighted CDE ($WCDE$) is reported with p -value (p) and 95% confidence intervals in brackets.

D.2 Liver Transplant Allocation

Additional Background The US liver transplant system has seen several key policy changes designed to optimize organ distribution and improve patient outcomes. In 2002, the *model for end-stage liver disease* (MELD) was adopted to determine patients' priority for liver transplants based on the severity of their illness (Malinchoc et al. 2000). In June 2013, UNOS implemented the *Share 35* policy to increase access to organs for patients with MELD scores ≥ 35 , given the high waitlist mortality in this subgroup (Wald et al. 2013). In January 2016, the MELD-sodium (i.e., MELD-Na) score incorporated serum sodium levels into the calculation (UNOS 2015). In February 2020, the acuity-circle (AC) policy for distributing livers replaced the longstanding donation service area-based policy (UNOS 2020). The AC policy uses a series of concentric circles, centered on the donor hospital, to determine the distribution range for available livers. In July 2023, the calculation formula for MELD was updated to include additional variables, including female sex and serum albumin (UNOS 2022). The new model, known as MELD 3.0, was expected to further refine the sorting of transplant candidates based on their medical urgency for transplant (Kim et al. 2021).

Data Preprocessing and Feature Selection We used the National Standard Transplant Analysis and Research (STAR) dataset for patient-level information on waitlisted transplant candidates, recipients, and donors from the Organ Procurement & Transplantation Network (OPTN) up to October 2022 (OPTN 2024). We filtered to include adult patients awaiting or having undergone a whole liver transplant from deceased donors in 2017-2019 and 2020-2022, keeping features relevant for discrimination discovery (Appendix D.2). Time frames were selected as stable periods without changes in the UNOS allocation policy.

We used the following features in the case study. Except for the liver allocation outcome, all features were determined at time of registration or listing. Thus, A1 holds. These features include all the possible parents to the liver allocation outcome available in the OPTN dataset, thus satisfying A2 to the best of our knowledge. For time period 2017-2019, total observations was $n = 21,101$ patients. For time period 2020-2022, total observations was $n = 22,807$ patients. Below, we provide the definition of each variable included in our causal analysis. Summary statistics are reported in Table D.6.

1. **Sex (exposure, protected attribute):** Recipient sex.
2. **Liver allocation (outcome):** Did the candidate receive a liver transplant?
3. **Recipient blood type:** Recipient blood group at registration.
4. **Initial age:** Age in years at time of listing.
5. **Ethnicity:** Recipient ethnicity category.
6. **Hispanic/Latino:** Is the recipient Hispanic/Latino?
7. **Education:** Recipient highest educational level at registration.
8. **Initial MELD:** Initial waiting list MELD/PELD lab score.
9. **Active exception case:** Was this an active exception case?
10. **Exception type:** Type of exception relative to hepatocellular carcinoma (HCC).
11. **Diagnosis:** Primary diagnosis at time of listing.
12. **Initial status:** Initial waiting list status code.
13. **Number of previous transplants:** Number of prior transplants that the recipient received.
14. **Weight:** Recipient weight (kg) at registration.
15. **Height:** Recipient height at registration.
16. **BMI:** Recipient body mass index (BMI) at listing.
17. **Payment method:** Recipient primary projected payment type at registration.
18. **Region:** Waitlist UNOS/OPTN region where recipient was listed or transplanted.

	UNOS POLICY (2017–2019)		UNOS POLICY (2020–2022)	
	LD3 ($\alpha = 0.01$)	LD3 ($\alpha = 0.05$)	LD3 ($\alpha = 0.01$)	LD3 ($\alpha = 0.05$)
\mathbf{A}_{DE}	active exception case, diagnosis, education, ethnicity, exception type, initial age, initial MELD, region, weight	active exception case, diagnosis, education, ethnicity, exception type, initial age, initial MELD, recipient blood type, region, weight	active exception case, diagnosis, education, ethnicity, initial age, initial MELD, payment method, region, weight	active exception case, diagnosis, education, ethnicity, initial age, initial MELD, payment method, region, weight
SDC	1	1	1	1
WCDE	0.033 [0.016,0.049]	0.025 [0.008,0.042]	0.032 [0.018,0.047]	0.032 [0.018,0.047]
p -value	0.000	0.003	0.000	0.000

Table D.2: Results obtained with nonparametric χ^2 independence tests and double machine learning. Total features is 18 (Appendix D.2). For time period 2017-2019, total observations is $n = 21101$ patients. For time period 2020-2022, total observations is $n = 22807$ patients. With no covariate control, SDC = 1 and the weighted CDE is 0.049 [0.033,0.066] (p -value = 0.000).

	UNOS POLICY (2017–2019)		UNOS POLICY (2020–2022)	
	PC ($\alpha = 0.01$)	PC ($\alpha = 0.05$)	PC ($\alpha = 0.01$)	PC ($\alpha = 0.05$)
\mathbf{A}_{DE}	education, recipient blood type	None	active exception case, initial MELD, recipient blood type	active exception case, initial age, recipient blood type, region
SDC	1	1	1	1
WCDE	0.046 [0.03,0.063]	0.049 [0.033,0.066]	0.037 [0.023,0.050]	0.028 [0.015,0.041]
p -value	0.000	0.000	0.000	0.000

Table D.3: SDC assessment and weighted CDE estimation with double machine learning using results from PC Algorithm (Spirites, Glymour, and Scheines 2001), as implemented by Kalisch and Bühlman (2007). We define \mathbf{A}_{DE} using the union method (PC_{\cup} ; Appendix C.2), though results for \mathbf{A}_{DE} were exactly the same using PC_{\cap} .

	UNOS POLICY (2017–2019)		UNOS POLICY (2020–2022)	
	LDECC ($\alpha = 0.01$)	LDECC ($\alpha = 0.05$)	LDECC ($\alpha = 0.01$)	LDECC ($\alpha = 0.05$)
\mathbf{A}_{DE}	payment method	payment method, region	active exception case, initial age, initial MELD, recipient blood type	diagnosis, recipient blood type, region
SDC	1	1	1	1
WCDE	0.049 [0.032,0.065]	0.048 [0.032,0.064]	0.032 [0.019,0.046]	0.032 [0.017,0.048]
p -value	0.000	0.000	0.000	0.000

Table D.4: SDC assessment and weighted CDE estimation with double machine learning using results from LDECC using the union method for selection \mathbf{A}_{DE} ($LDECC_{\cup}$; Appendix C.2) (Gupta, Childers, and Lipton 2023). Results for \mathbf{A}_{DE} were almost concordant using $LDECC_{\cap}$, with the exception of 2020-2022 when $\alpha = 0.05$ (where the intersection method excluded diagnosis).

Policy	α	LD3		LDECC		PC		RATIO PC/LD3		RATIO LDECC/LD3	
		Time	Tests	Time	Tests	Time	Tests	Time	Tests	Time	Tests
2017-2019	0.01	0.100	75	20.304	3303	237.324	35943	2373.24	479.24	203.04	44.04
	0.05	0.101	75	19.947	3188	231.844	36512	2295.48	486.83	197.50	42.51
2020-2022	0.01	0.107	75	47.402	6959	465.278	63225	4348.39	843.00	443.01	92.79
	0.05	0.090	71	519.707	69926	528.372	72517	5870.80	1021.37	5774.52	984.87

Table D.5: Total number of independence tests performed and runtimes in seconds for LD3 vs PC (Kalisch and Bühlman 2007) and LDECC (Gupta, Childers, and Lipton 2023) on the liver transplant allocation dataset. While PC is worst-case exponential in time complexity (Spirtes, Glymour, and Scheines 2001), LDECC is worst-case exponential for some structures and polynomial for others (Gupta, Childers, and Lipton 2023). This could explain the wide variation in LDECC runtimes across experimental settings.

	UNOS POLICY (2017-2019)			
	Female (n = 7679)	Male (n = 13422)	p-value	Test
Active exception case	0.36 (0.73)	0.48 (0.83)	7.241e-28	t-test
Diagnosis 1 (PSC: Primary Sclerosing Cholangitis)	0.03 (0.18)	0.04 (0.2)	0.037	χ^2
Diagnosis 6 (AHF: acute hepatic failure)	0.06 (0.23)	0.02 (0.15)	0.004	χ^2
Diagnosis 7 (Cancer)	0.09 (0.28)	0.16 (0.37)	0.010	χ^2
Height	161.9 (7.46)	175.91 (8.51)	0.000	t-test
Initial MELD	20.5 (10.21)	18.83 (9.87)	1.588e-31	t-test
Payment method	0.53 (0.5)	0.54 (0.5)	0.012	χ^2
Recipient age	54.46 (12.42)	56.03 (10.74)	4.091e-22	t-test
Weight	75.97 (18.53)	90.63 (19.59)	0.000	t-test
	UNOS POLICY (2020-2022)			
	Female (n = 8574)	Male (n = 14233)	p-value	Test
Active exception case	0.39 (0.58)	0.43 (0.63)	3.629e-07	t-test
Ethnicity 9 (Multiracial, non-hispanic)	0.01 (0.08)	0.0 (0.07)	0.022	Fisher's exact
Exception type 1 (Unknown)	0.29 (0.45)	0.28 (0.45)	0.022	χ^2
Height	161.96 (7.8)	176.36 (8.25)	0.000	t-test
Initial MELD	22.13 (10.52)	20.99 (10.48)	1.862e-15	t-test
Initial status	0.04 (0.2)	0.02 (0.12)	2.858e-31	t-test
Recipient age	53.83 (12.75)	54.74 (11.64)	3.059e-08	t-test
Weight	75.76 (18.71)	91.1 (20.32)	0.000	t-test

Table D.6: Mean values (standard deviations) for features with statistically significant differences between males and females ($\alpha = 0.05$). Summary statistics for all features are available on GitHub (<https://anonymous.4open.science/r/LD3-4440>).